Some Application of Laser-Compton Scattering from Intermediate Energy Electron Beams

K. Chouffani

Idaho Accelerator Center, Idaho State University, Pocatello, ID 83209.

Laser-Compton Scattering (LCS)

- Interaction of high-energy electron with photon $\Rightarrow$ electron scatters low energy photon to higher energy at the expense of the electron kinetic energy.
- Similar to channeling/Undulator radiation
- Emission of highly directed (direction of e- beam), mono-energetic, and tunable X-ray beams with divergence on the order of $1/\gamma$.

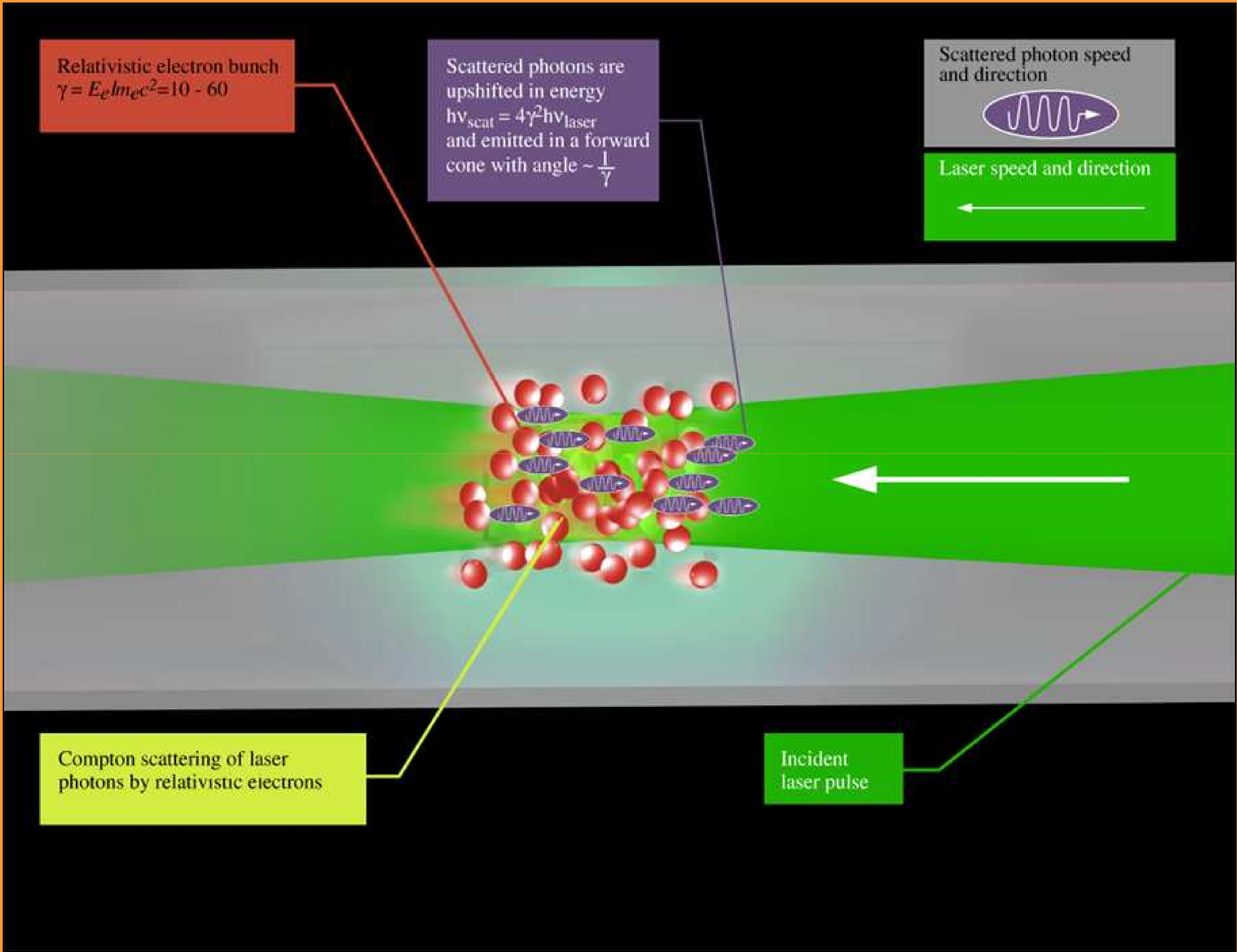

Relativistic electron bunch
$\gamma = E_e/m_e c^2 = 10 - 60$
Scattered photons are upshifted in energy
$h\nu_{scat} = 4\gamma^2 h\nu_{laser}$
and emitted in a forward cone with angle $\sim \frac{1}{\gamma}$
Scattered photon speed and direction
Laser speed and direction
Compton scattering of laser photons by relativistic electrons
Incident laser pulse

- Compton x-ray energy (from energy momentum conservation):

$$E_\gamma \approx \frac{E_L(1+\beta\cos\alpha)}{1-\beta\cos\theta}.$$

- E_γ = x-ray energy, E_L = Laser photon energy, E_B = Electron beam total energy.
- For collision geometries were $\alpha \approx 0$ and for emission angles close to the electron beam direction:

$$E_\gamma \approx E_M \big/ (1+\gamma^2\theta^2).$$

- Where $E_M = 4\gamma^2 E_L$ is the maximum energy generated in the forward direction for a head-on collision (Highest gain in energy, twice Doppler shifted).

LCS Spectrum

Laser photon energy in e- frame $<< mc^2$ ==> motion of e- is non-relativistic (Thomson scattering).

Energy of incoming photon = energy of scattered photon in rest frame

Rest frame differential cross section (for an incident linearly polarized plane wave):

$$\frac{d\sigma}{d\Omega'} = r_0^2 \sum \left| \vec{\varepsilon}_l^{\,'} . \vec{\varepsilon}_\gamma^{\,'} \right|^2 = r_0^2 (\cos^2\theta' \cos^2\varphi' + \sin^2\varphi')$$

After transformation to laboratory frame (laser polarization along x axis)

$$\frac{d\sigma}{d\Omega} = r_0^2 \frac{1-\beta^2}{(1-\beta\cos\theta)^2} \left(\cos^2\varphi \frac{(\cos\theta - \beta)^2}{(1-\beta\cos\theta)^2} + \sin^2\varphi \right)$$

$$\frac{\mathrm{d}N_\gamma}{\mathrm{d}E_\gamma} = \int_{\mathrm{d}\Omega_d} \frac{\mathrm{d}N_\gamma}{\mathrm{d}\Omega_d\,\mathrm{d}E_\gamma}\,\mathrm{d}\Omega_d\,,$$

$$\frac{\mathrm{d}N_\gamma}{\mathrm{d}\theta_{x,d}\mathrm{d}\theta_{y,d}\mathrm{d}E_\gamma} = L\frac{\mathrm{d}\sigma}{\mathrm{d}\theta_{x,d}\mathrm{d}\theta_{y,d}\mathrm{d}E_\gamma}$$

$$= \frac{L\,2r_0^2}{(2\pi)^{3/2}\,\sigma_x\sigma_y\sigma_e}\int_0^\infty\int_0^{2\pi}\frac{(1+\beta)}{E_M}\left[(\cos 2\varphi+1)\frac{E_\gamma}{E_M}\left(\frac{E_\gamma}{E_M}-1\right)+1/2\right]$$

$$\mathrm{x}\exp\left(-\frac{(\gamma'-\gamma)^2}{2\sigma_e^2}\right)\exp\left(-\frac{(\theta_{x,d}-\theta_x)^2}{2\sigma_x^2}\right)\exp\left(-\frac{(\theta_{y,d}-\theta_y)^2}{2\sigma_y^2}\right)\mathrm{d}\varphi\,\mathrm{d}\gamma'.$$

$\mathrm{d}\Omega_d = \mathrm{d}\theta_{x,d}\mathrm{d}\theta_{y,d}$, $\theta_{x,d} \approx \theta_d\cos\varphi_d$, $\theta_{y,d} \approx \theta_d\sin\varphi_d$,

$\theta_x \approx \theta\cos\varphi$, $\theta_y \approx \theta\sin\varphi$, $E_M = 4\gamma'^2 E_L$ and $\theta \approx \sqrt{(E_M/E_\gamma - 1)}/\gamma'$.

L: single collision luminosity.

Assume transverse and longitudinal spatial distributions are Gaussians:

If laser pulse length much shorter than Rayleigh range and e- beam envelope function greater than e- pulse length, transverse rms widths considered independent of longitudinal coordinate and sinα ≈ α (laser propagates in the *y*-*z* plane) :

$$L = \frac{N_e N_L (1+\beta)}{2\pi\alpha c \sigma_\tau \sqrt{x_\sigma^2 + \sigma_w^2}} \exp(-\tau^2 / 2\sigma_\tau^2),$$

$$\sigma_\tau = ((1+\beta)/\alpha c)\sqrt{(\alpha/(1+\beta))^2 (z_\sigma^2 + \sigma_L^2) + (y_\sigma^2 + \sigma_w^2)}$$

τ: delay between laser and electron beam

For α = 0

$$L = N_e N_L \Big/ 2\pi \sqrt{x_\sigma^2 + \sigma_w^2}\,\sqrt{y_\sigma^2 + \sigma_w^2}$$

Number of LCS X-rays/burst:

$N_{LCS} = L\, \sigma_\Omega(\sigma_x, \sigma_y)$, σ_Ω = Cross section within cone of solid angle Ω.

LCS x-ray energy and energy spread (FWHM) depend on

- Laser frequency bandwidth.
- Electron beam energy and energy deviation.
- e- beam angular spread.
- Electron beam direction.
- Finite detector collimation.
- Finite interaction length.

Potential applications of LCS

- LCS x-ray pulse durations:

- 180^o geometry: $\tau_x \approx \tau_e$

- 90^o geometry: τ_x = transit time

- 90^o LCS geometry: scanning laser across e-beam spot size (nm range).

- Electron beam emittance, energy, energy spread and direction.

Spectral bandwidth vs collimator radius

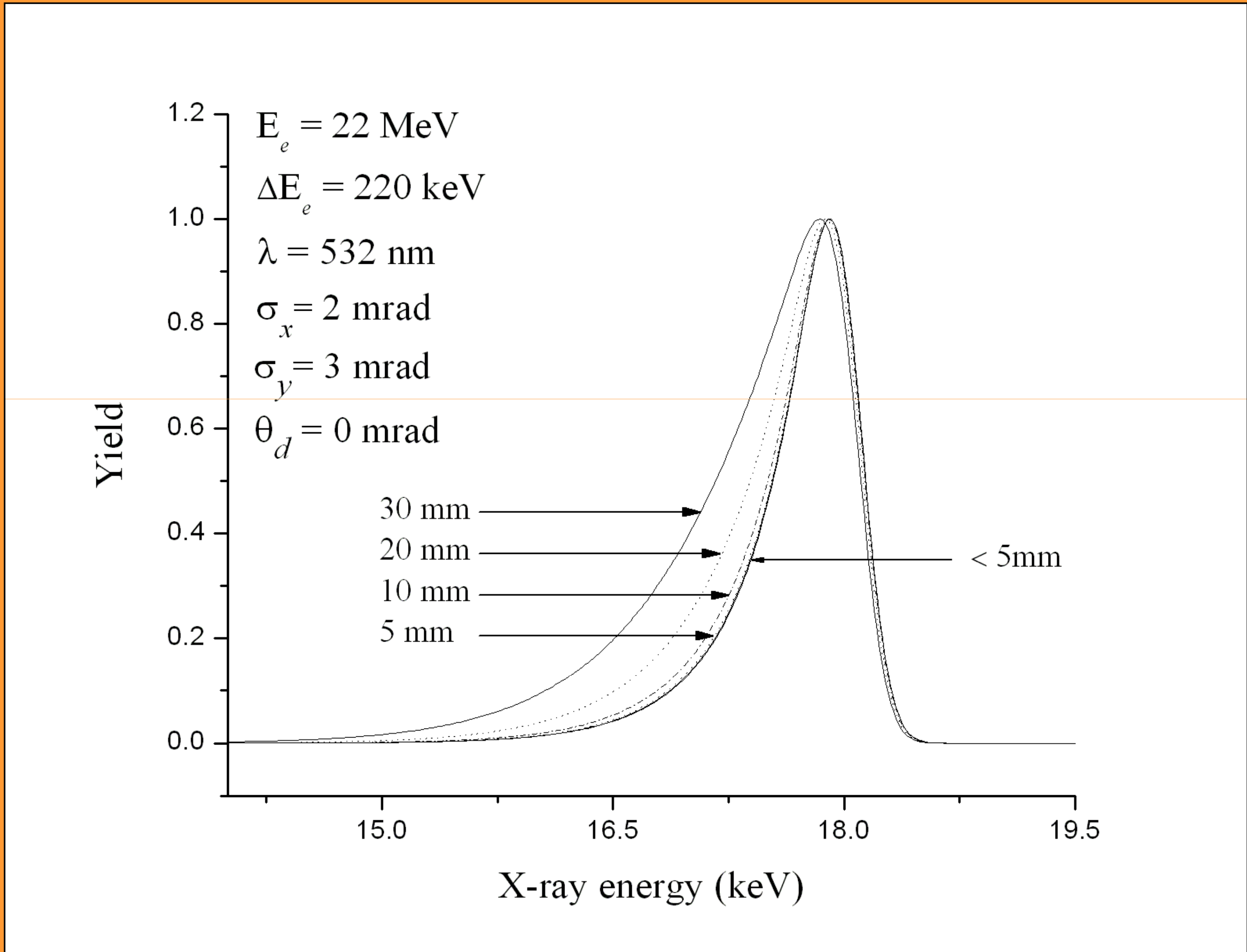

LCS energy and FWHM dependence on beam divergence σ_x and σ_y for scans along x-direction (laser electric field)

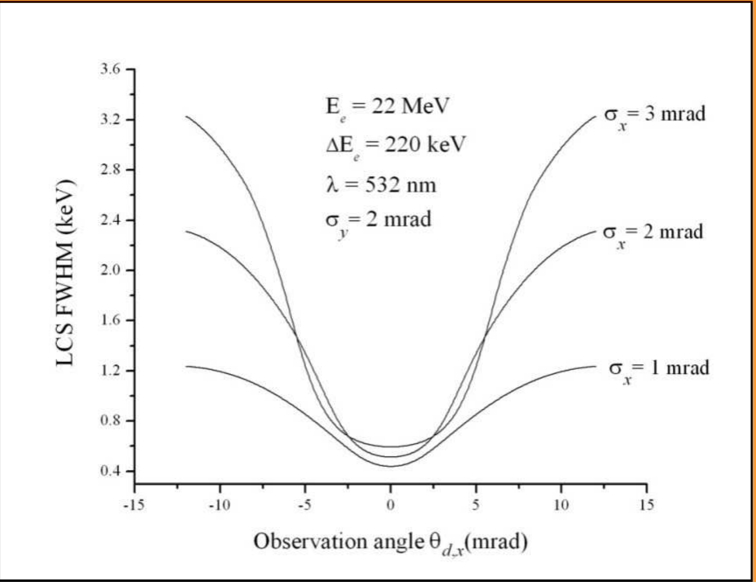

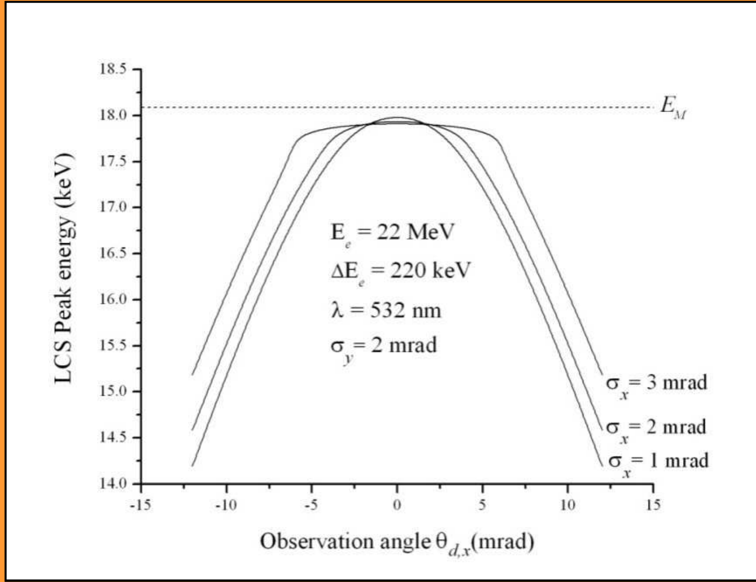

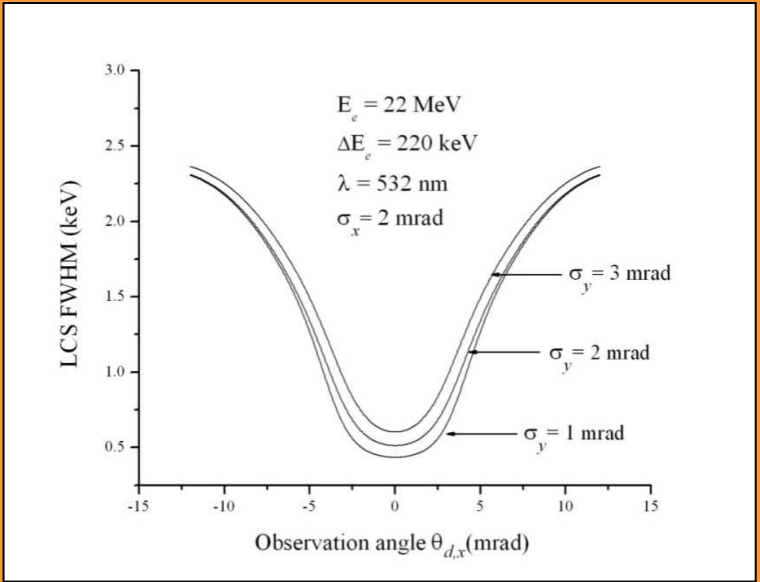

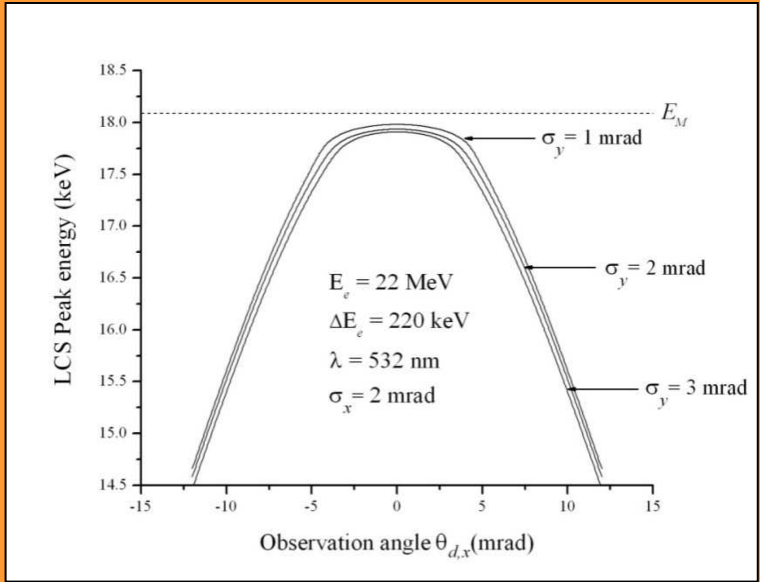

IAC L-band LINAC Layout

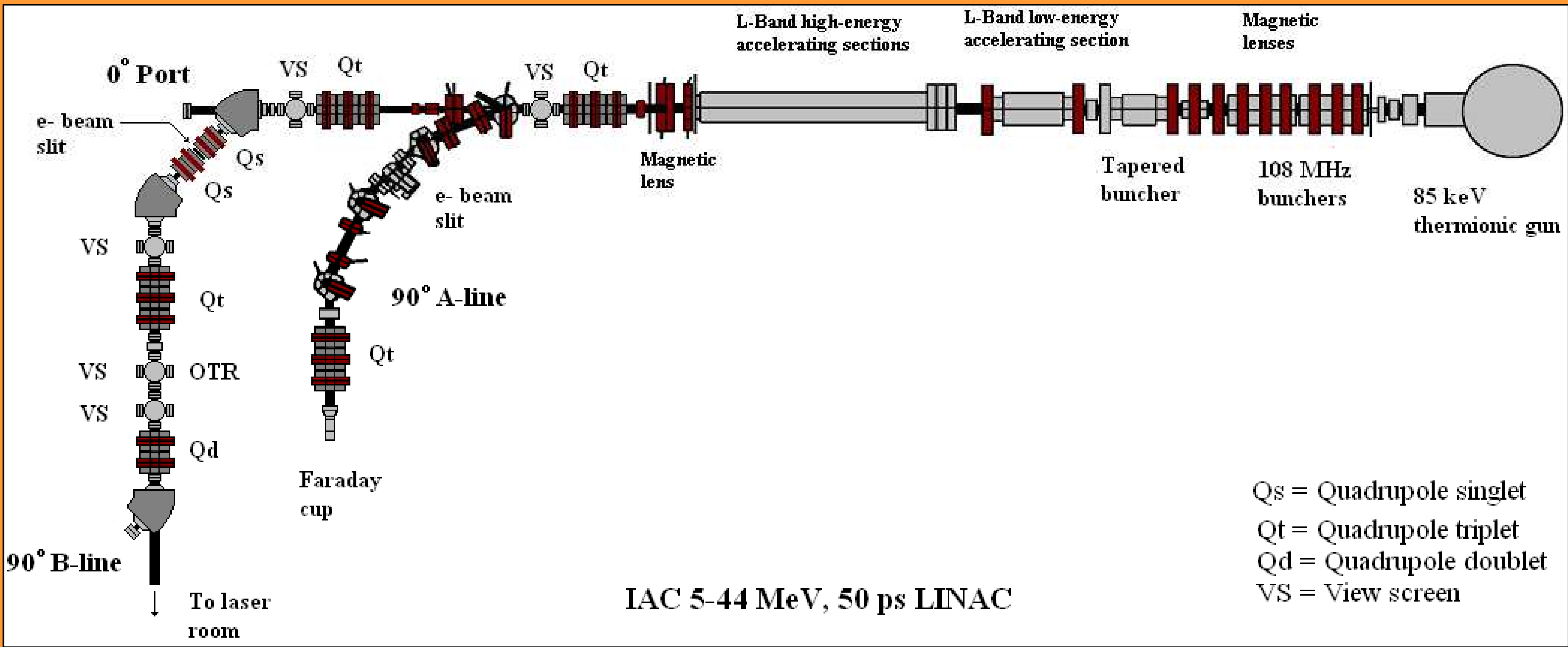

Electron beam and laser parameters (LCS-Experiment) B-Line

- <u>Electron beam:</u>
- Beam energy:
  5-44 MeV
- Pulse length: 50 ps
- Charge/bunch
  up to 10 nC.
- Typical bunch charge=
  0.35 nC
- Rep. Rate = 60 HZ

- <u>YAG-Laser:</u>
- Fundamental
  λ_1 = 1064 nm +second,
  third and fourth harmonic
- Pulse length = 250 ps
- E_1= 1 J/pulse
- E_2 = 500 mJ/pulse
- E_4 = 33 mJ/pulse
- Rep. Rate = 60 HZ

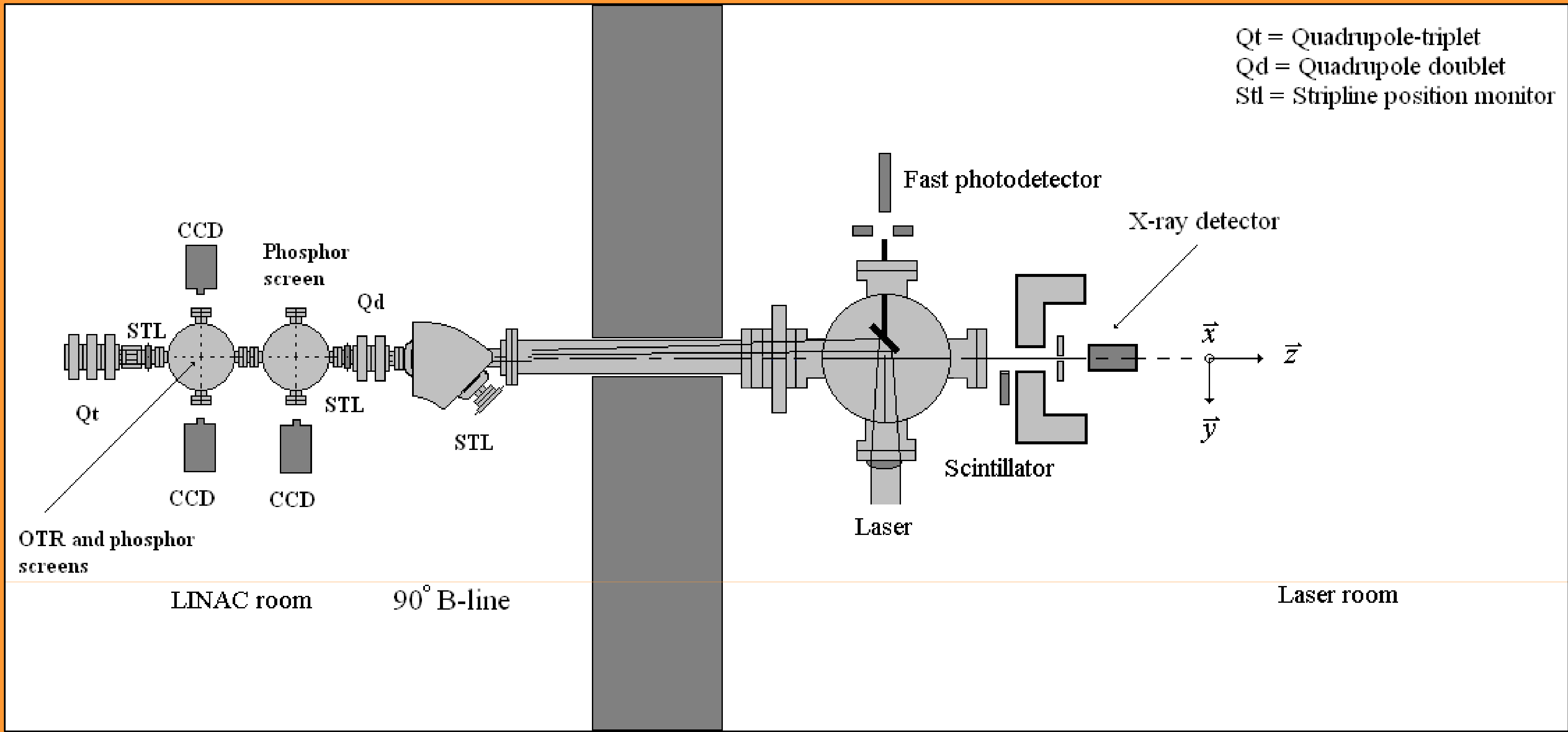

- Laser-beam line angle:α ≅ 2.2 mrad.
- Solid angle: $d\Omega_\gamma \cong 0.2$ μsr.
- 1064 nm-Pol: π, 532 nm-Pol: σ, 266 nm-Pol: π
- Seed laser phase locked to Linac 108 MhZ clock.

Jitter e-beam and laser ≅ 1ps

Laser Room (4 GW, 60 Hz, 250 ps Nd:YAG)

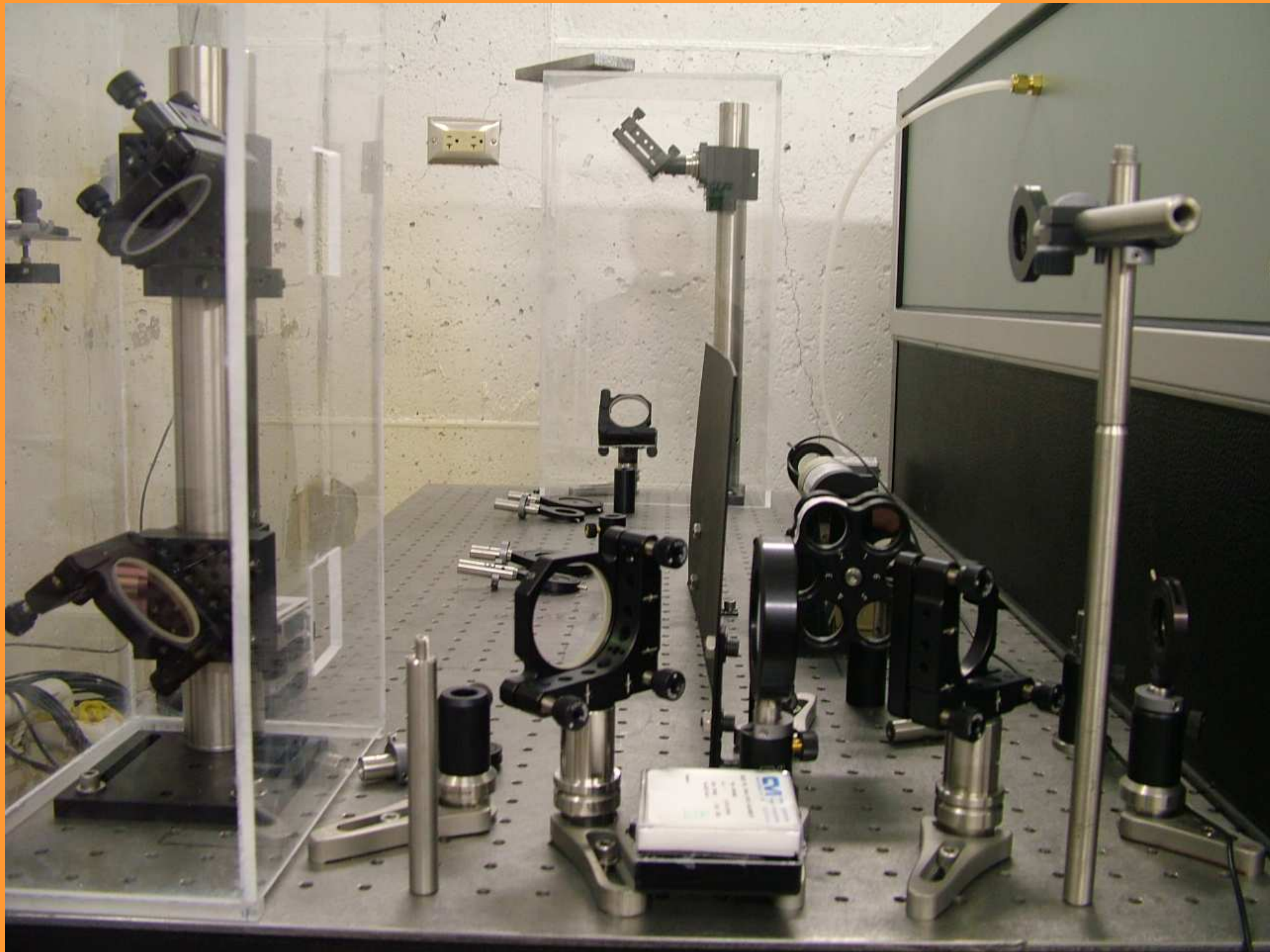

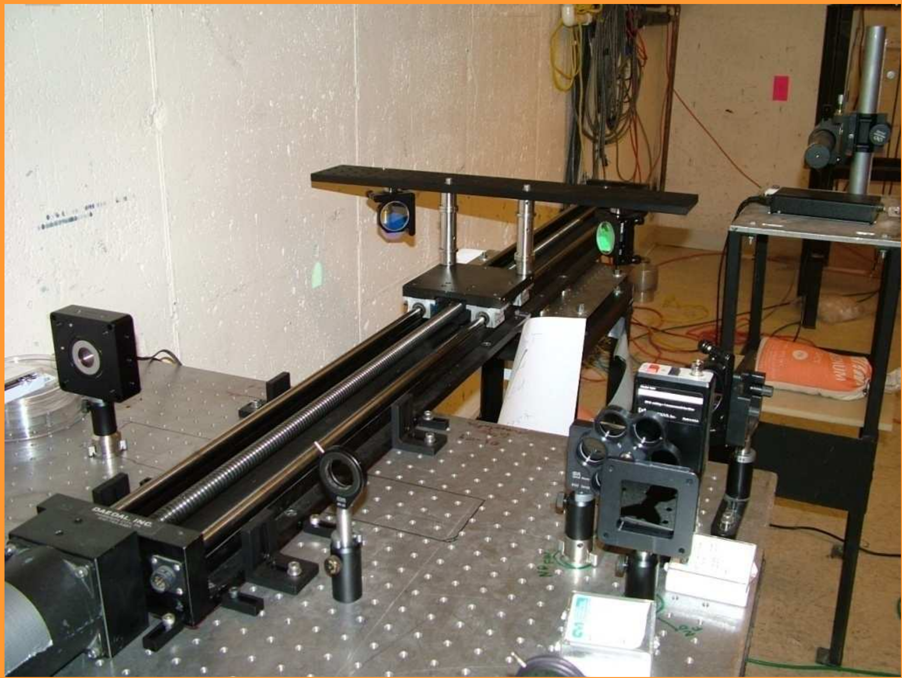

Optics room:

Prior to injecting laser

to interaction area

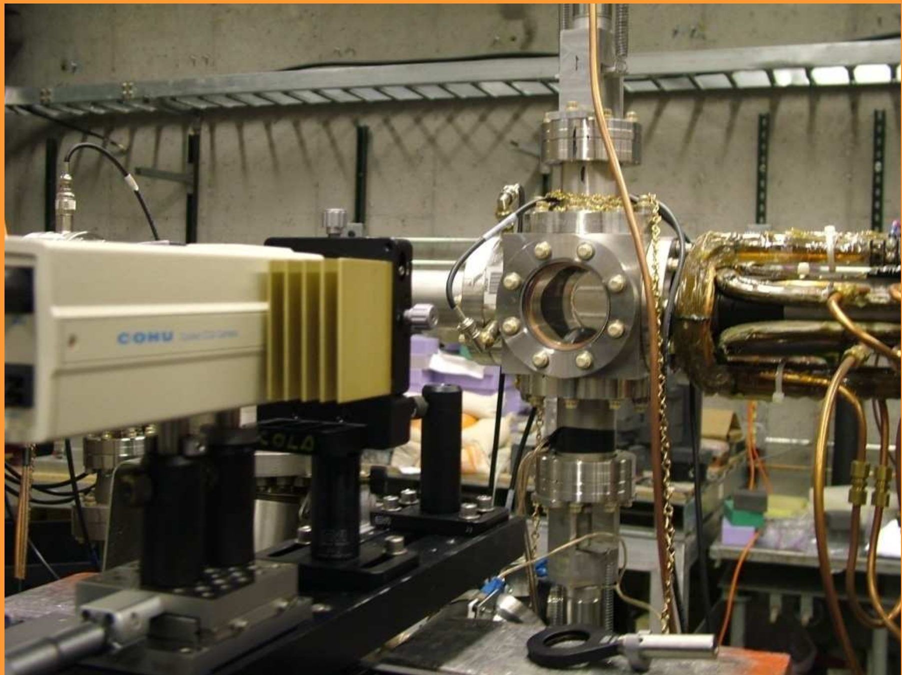

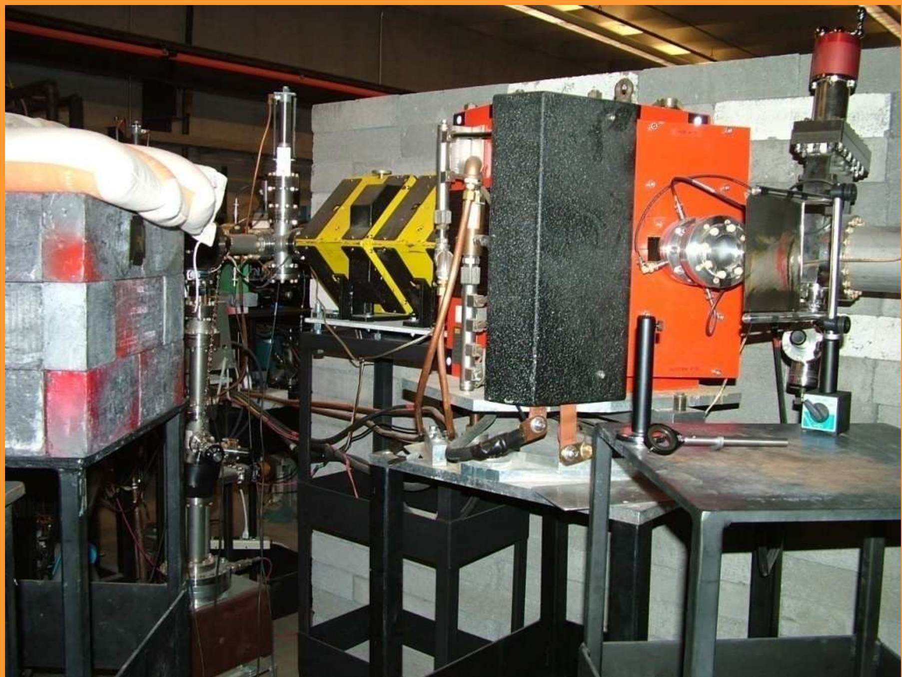

Inside LINAC room

e- beam-laser pulses
temporal overlap:
a-Discreet jumps *i.e.* 9.26 ns
b-Seed laser phase *i.e.* 4.6 ns
c-Translator *i.e.* 9.26 ns
(2x1.7 m)

Delay between laser and e- beam pulses

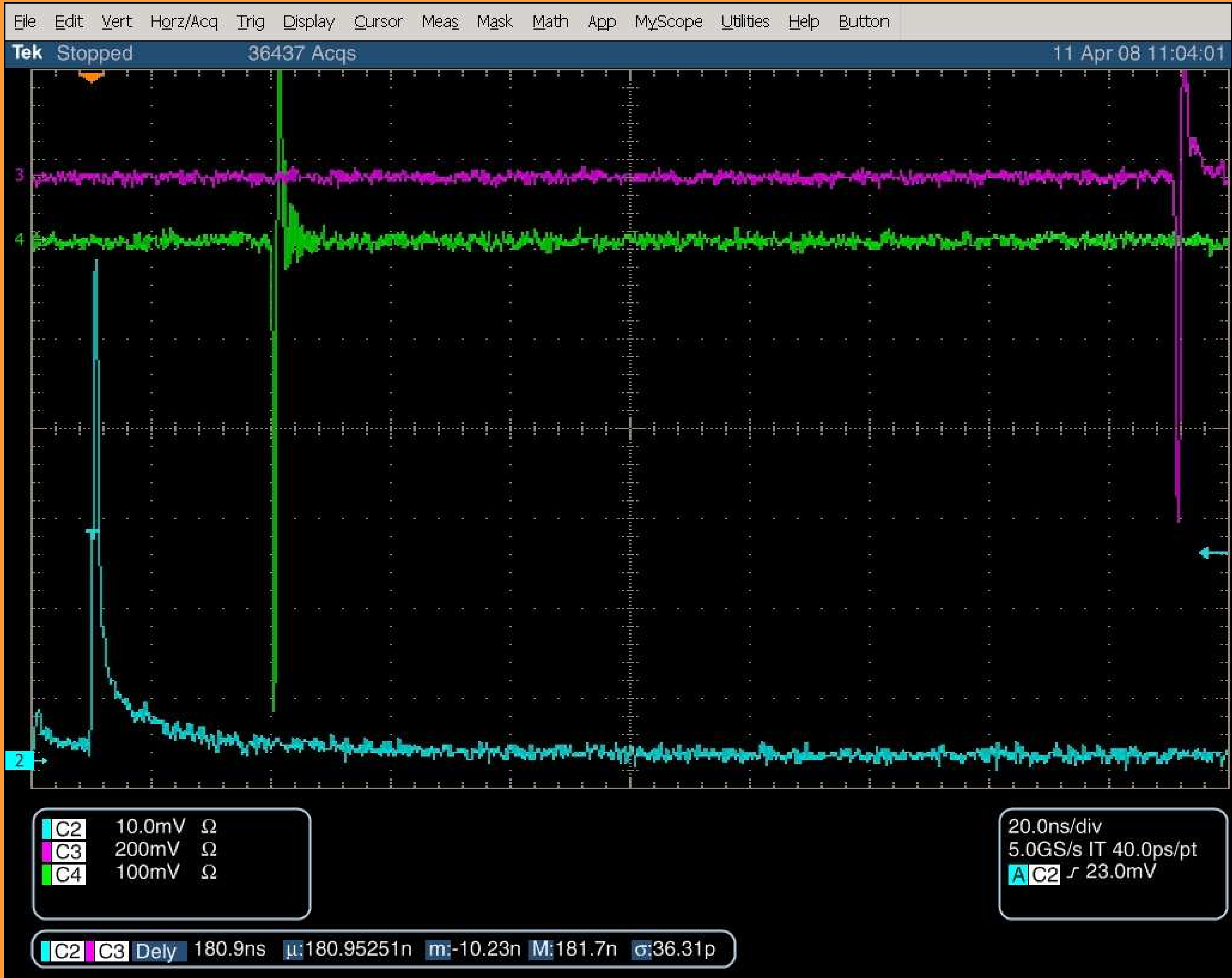

Rms spot size at interaction

e^- beam (depends on bunch charge):

$x_\sigma = 1.95 \pm 0.02$ mm

$y_\sigma = 0.625 \pm 0.004$ mm

Laser (depends on optics and wavelength)

$x_\sigma = 82.6 \pm 0.1\ \mu m$

$y_\sigma = 154.3 \pm 0.4\ \mu m$

τ_e =50 ps, τ_L =250 ps Q = 0.35 nC, laser, E_L = 50 mJ, α = 2.5 mr, dΩ = 0.25 μSr, N_{LCS} = 2.76 ± 0.02

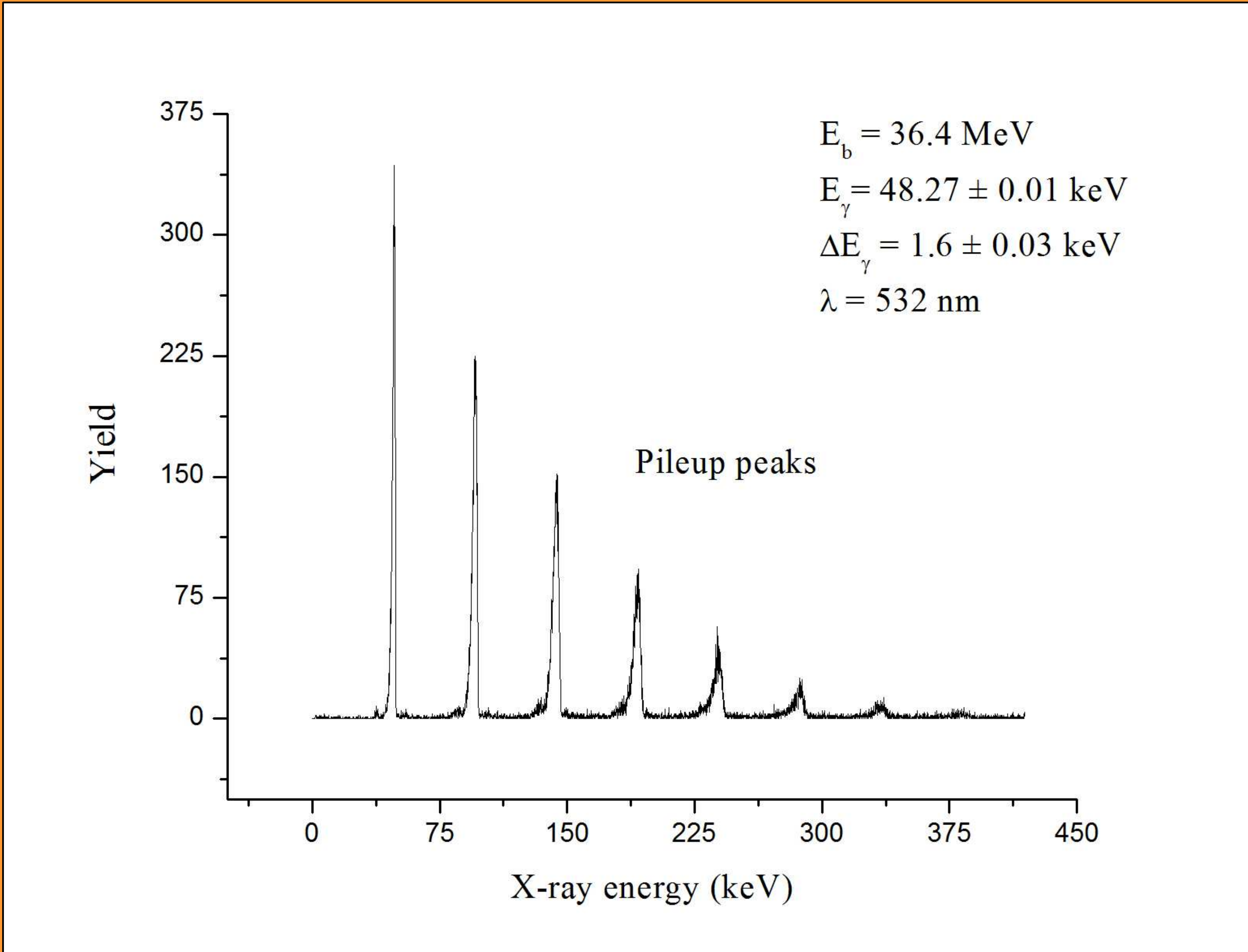

Pileup energy distribution

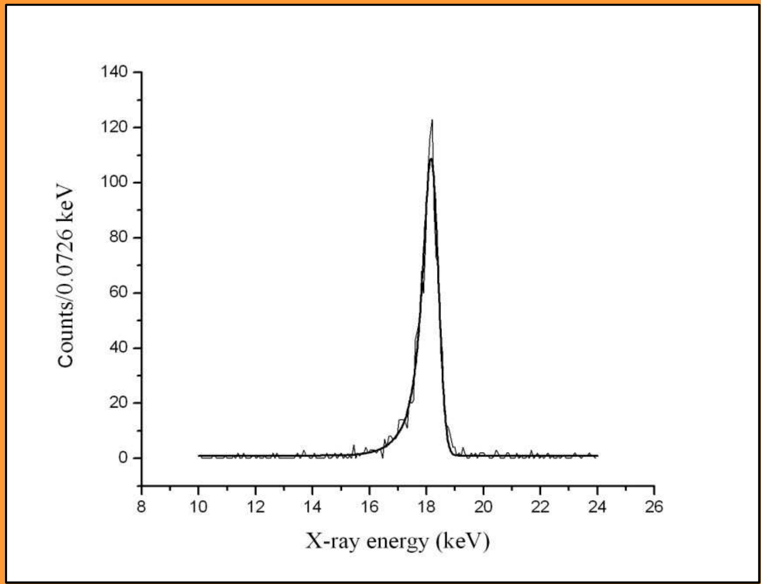

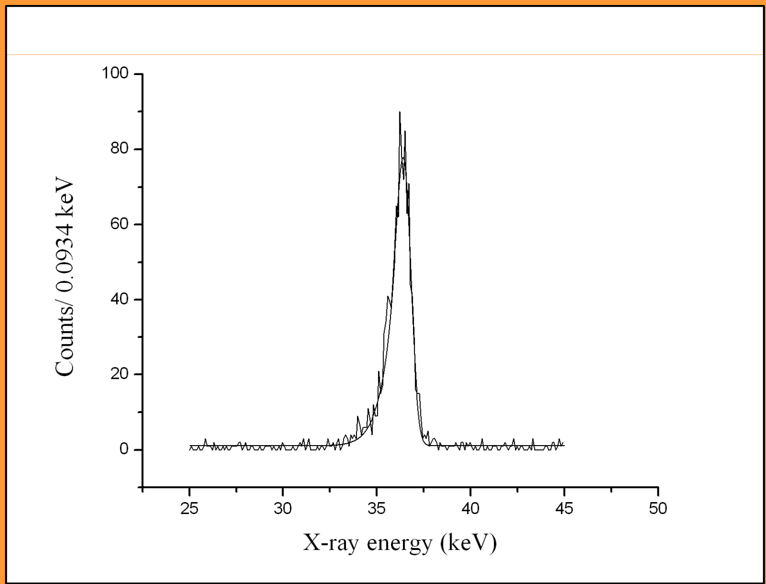

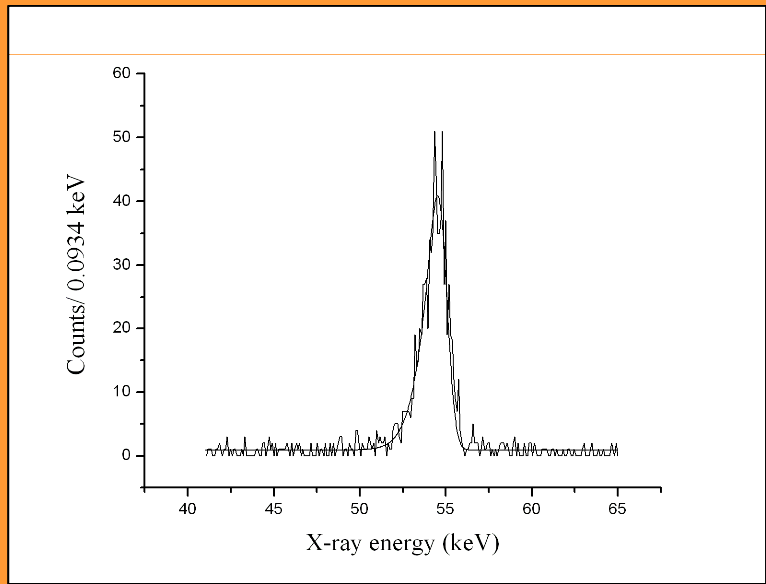

$$g(E_\gamma) = \int f(E'_\gamma)\, f(E_\gamma - E'_\gamma)\, \mathrm{d}\, E'_\gamma$$

$$h(E_\gamma) = \iint f(E''_\gamma)\, f(E'_\gamma - E''_\gamma)\, f(E_\gamma - E'_\gamma)\, \mathrm{d}\, E''_\gamma\, \mathrm{d}\, E'_\gamma$$

τ_e =5 ns, τ_L = 7 ns, $Q_{macropulse}$ = 0.2 nC, laser, E_L = 200 mJ, Slit width = 3.4 mm

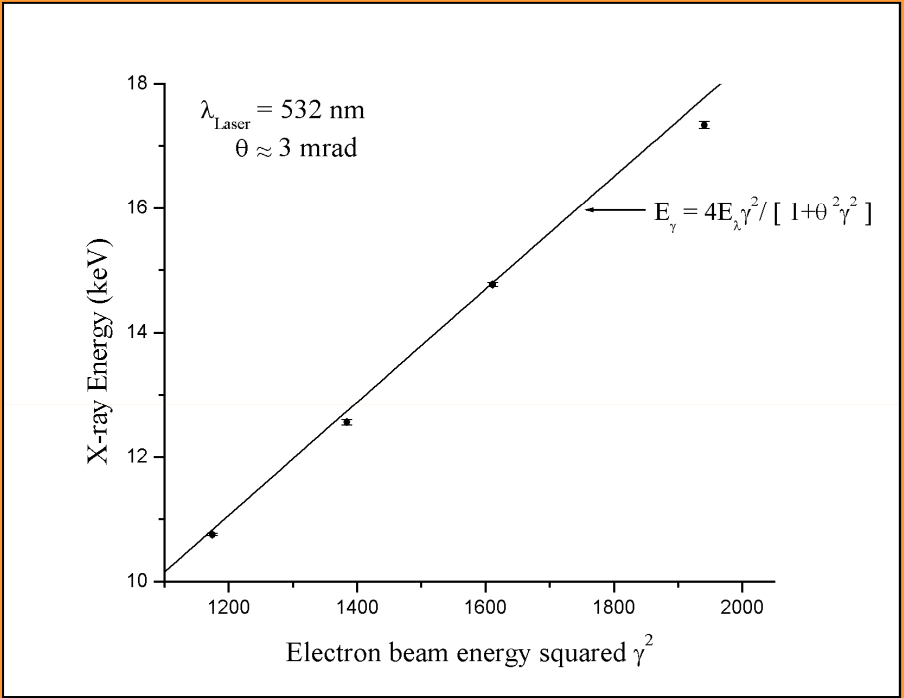

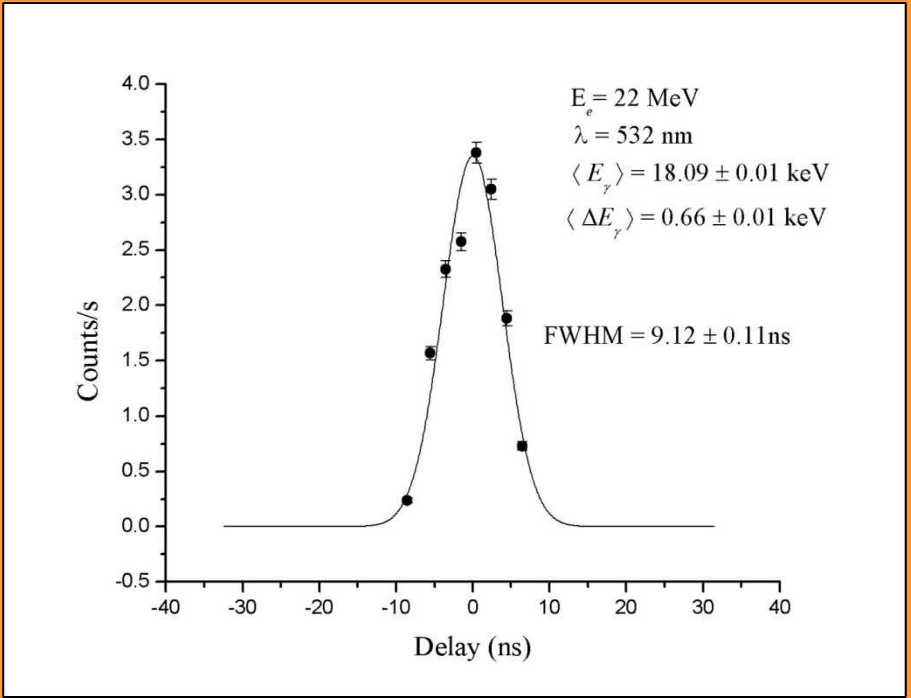

LCS energy tunability

Time delay between laser and electron beam pulses

Basic application of LCS

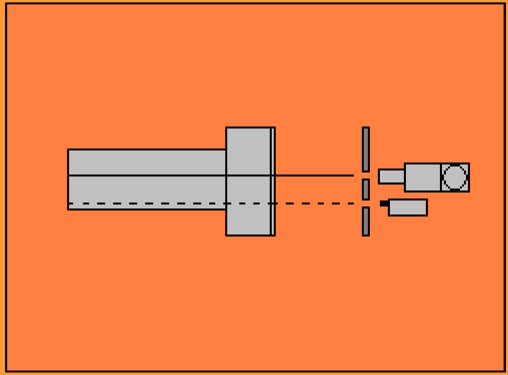

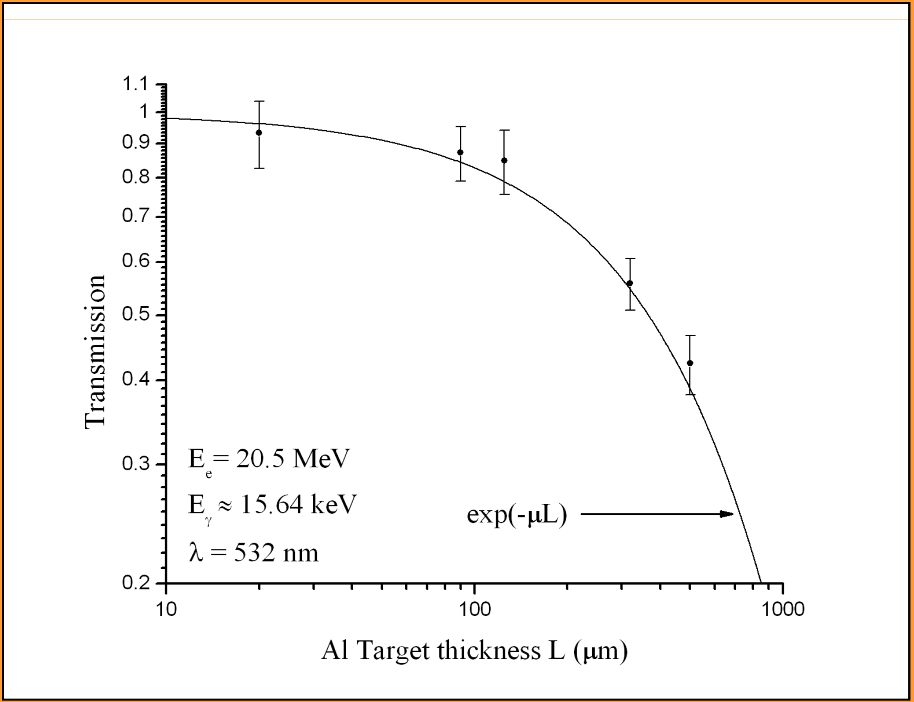

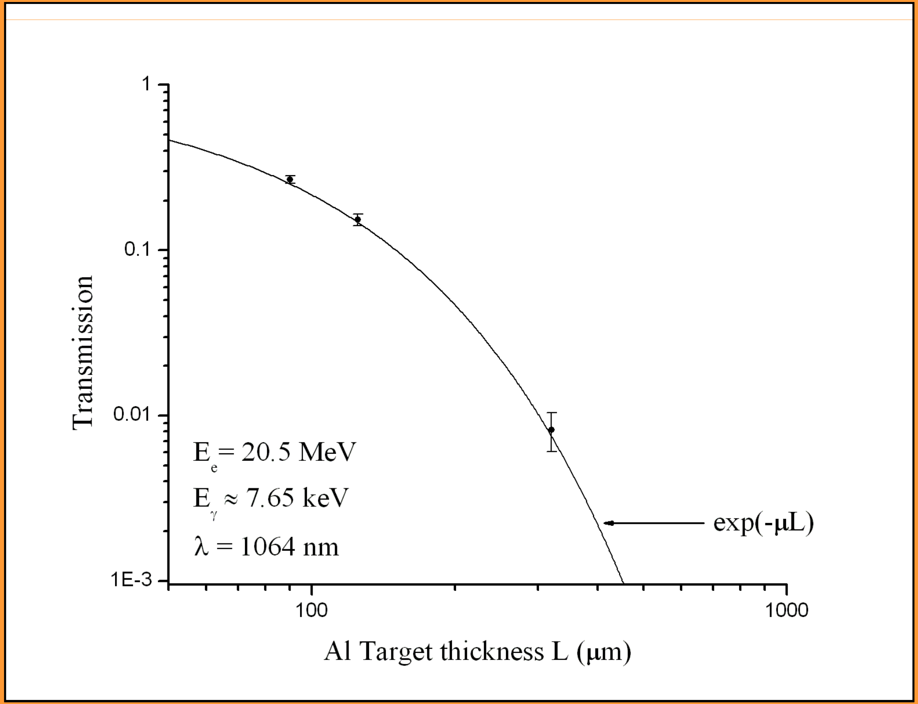

LCS as a non-invasive beam diagnostics technique: Angular measurements

- Scan across x-ray cone along horizontal and vertical directions.

Minimization method:

- Common fit to spectra to determine common e-beam Parameters from several responses *i.e.* spectra.
- Minimization of det $\{V_{i,j}\}$

$$\{V_{i,j}\} = \sum_k \frac{(y_{i,k} - f_{i,k})}{\sigma_{i,k}} \frac{(y_{j,k} - f_{j,k})}{\sigma_{j,k}}$$

Measured beam parameters with minimization method

With 15 spectra:

$E = 22.27 \pm 0.04$ MeV

$\Delta E = 0.21 \pm 0.07$ MeV

$\sigma_x = 2.08 \pm 0.13$ mrad

$\sigma_y = 3.05 \pm 0.5$ mrad

$\theta_b = -2.12 \pm 0.32$ mrad.

With energy and FWHM (E and ΔE fixed)

$\sigma_x = 2.23 \pm 0.11$ mrad

$\sigma_y = 2.81 \pm 0.5$ mrad

$\theta_b = -2.15 \pm 0.5$ mrad.

K. Chouffani *et al*. Laser Part. Beams 24, (2006) 411, Phys. Rev. Spec. Top. AB 9, 050701 (2006).

LCS Energy, FWHM VS Observation angle

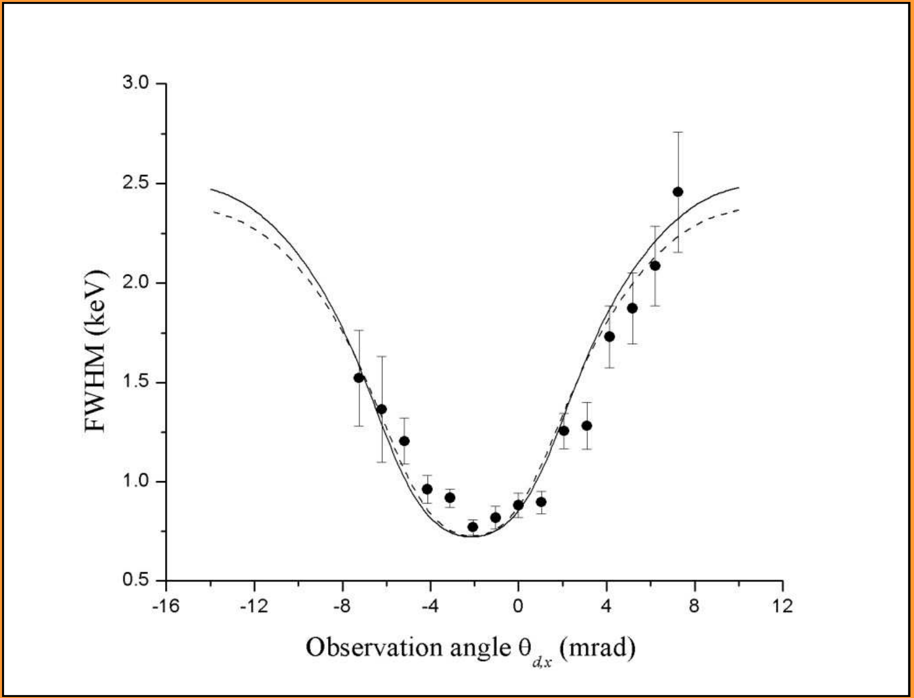

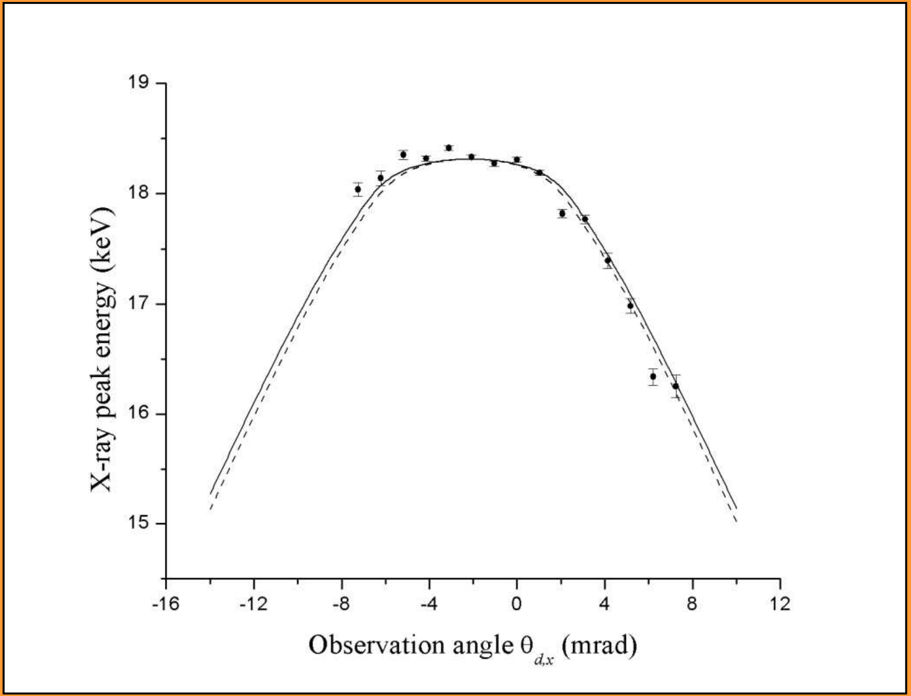

LCS for non-proliferation ➔ Hybrid K-edge densitometry (HKED) ➔Identifications and quantification (concentration/concentration ratio) of actinide elements in liquid samples.

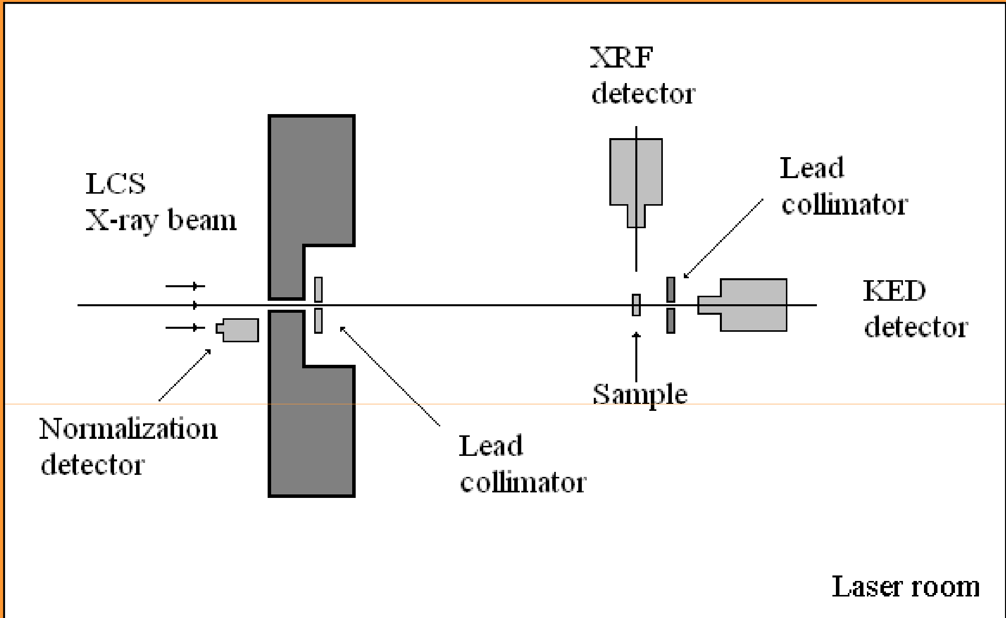

Need to reach 42.3 MeV ==>
E_γ = 129.5 keV > k-edges of 238U, 237Np, 239Pu, 241Am and 244Cm (128.2 keV).

KED utilizes abrupt change in x-ray transmission at the k absorption edge of a certain heavy element in order to determine its concentration.

XRF determines various ratios of concentrations (U/Pu). Measured ratios allow determination of each minor element relative to major elements and therefore after appropriate calibration allow determination of absolute concentration of a minor element.

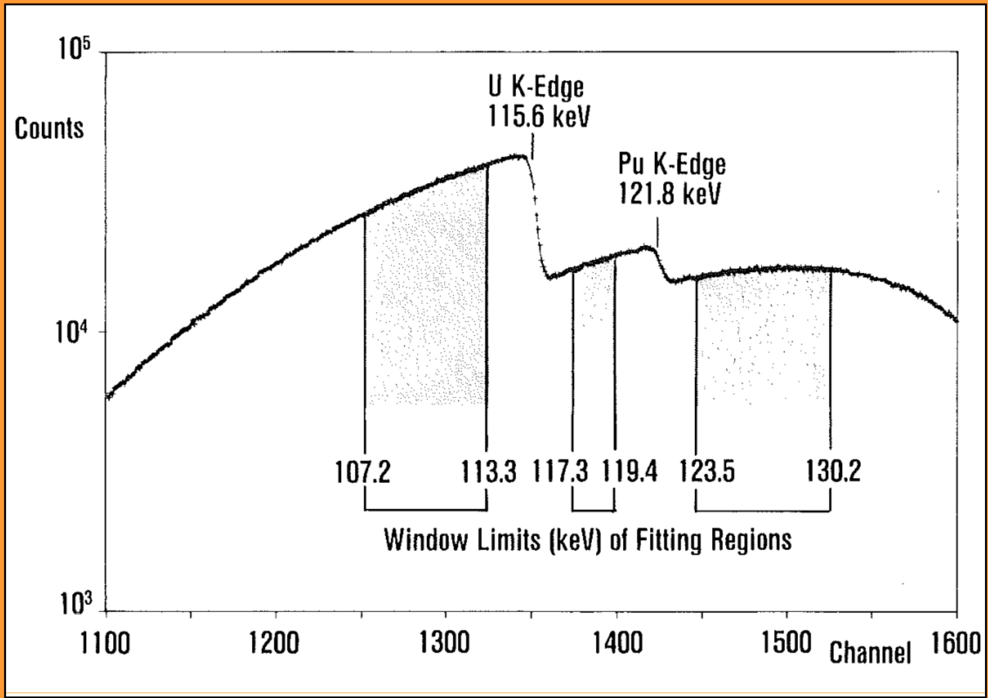

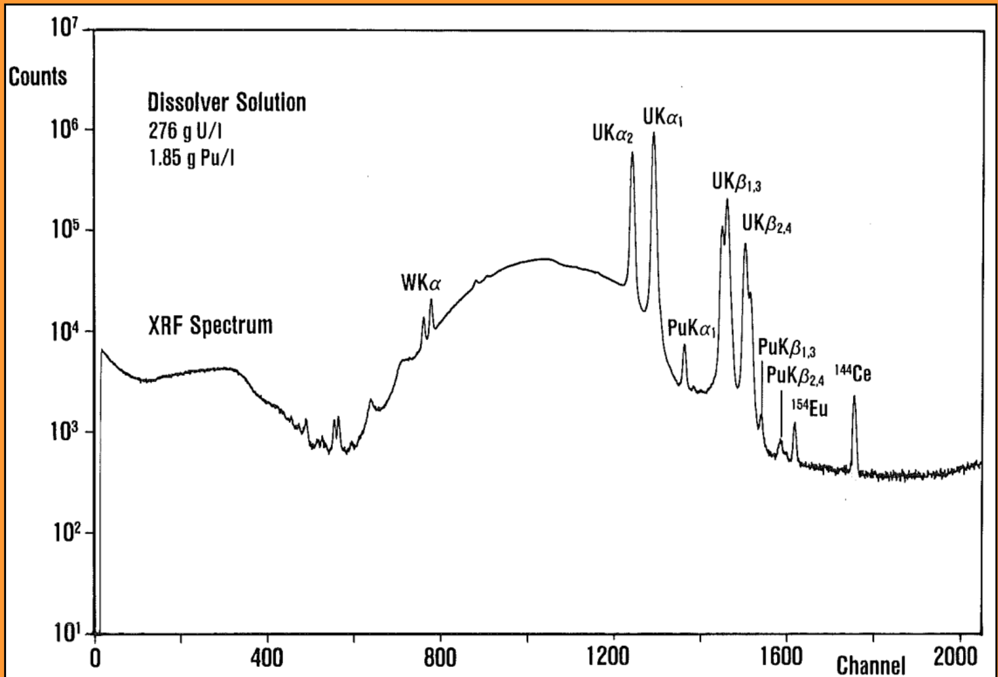

Ottmar *et al.*
Hybrid K-edge densitometry with bremsstrahlung beams:
*150 kV/15 mA X-ray tube.
*2 high purity Germanium detectors.
*XRF detector at 150^o with respect to primary direction of X-ray beam. Lots of useless photons and poor signal to noise ratio.

3 M Nitric acid solution (reference solution), Path length = 2 cm, Volume = 7ml, 1.08g/cm^3 E beam energy =42.5 MeV, Laser energy = 3 mJ

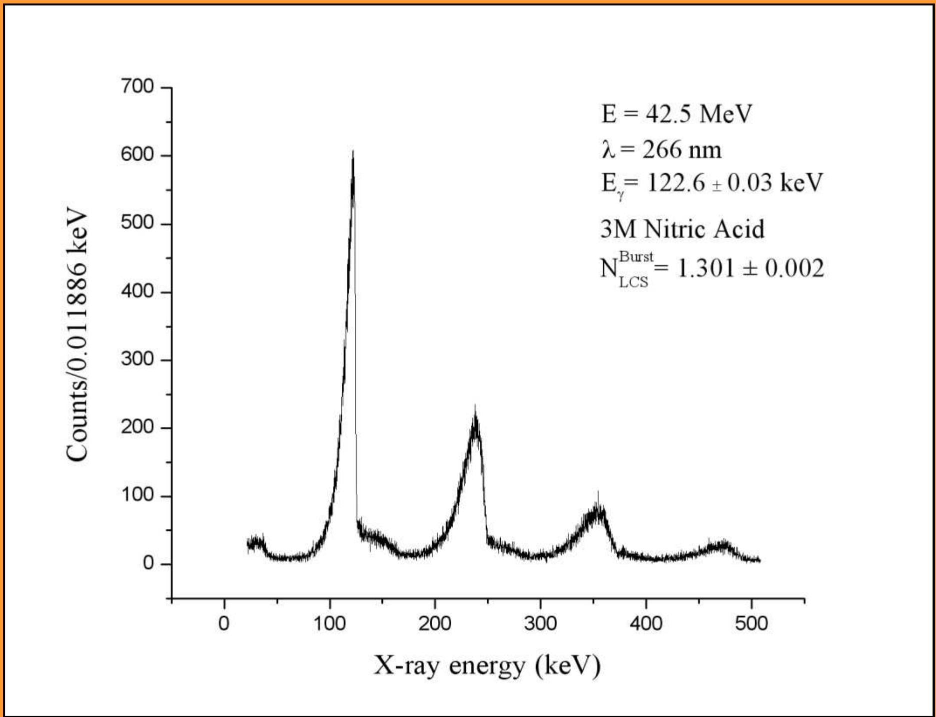

Samples provided by Sandia National Laboratory

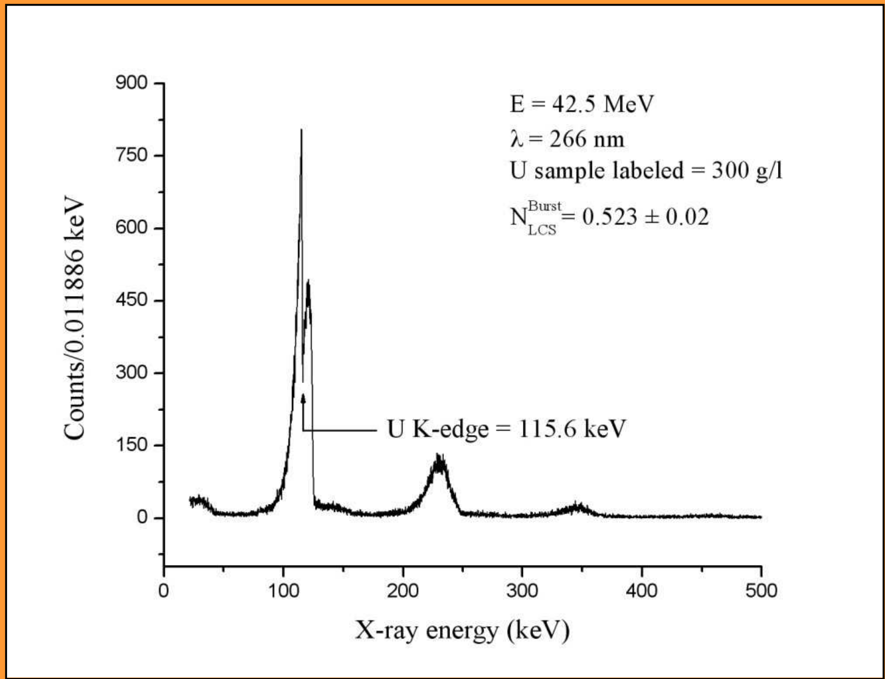
E = 42.5 MeV
λ = 266 nm
U sample labeled = 300 g/l
N_{LCS}^{Burst} = 0.523 ± 0.02
U K-edge = 115.6 keV
Counts/0.011886 keV
X-ray energy (keV)
900
750
600
450
300
150
0
0
100
200
300
400
500

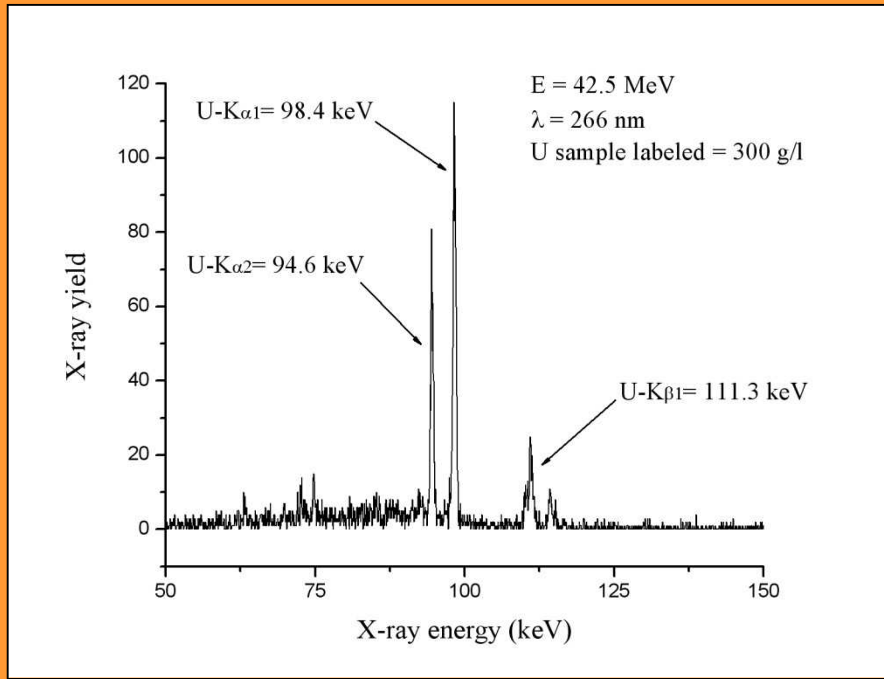
E = 42.5 MeV
λ = 266 nm
U sample labeled = 300 g/l
U-Kα1= 98.4 keV
U-Kα2= 94.6 keV
U-Kβ1= 111.3 keV
X-ray yield
X-ray energy (keV)
120
100
80
60
40
20
0
50
75
100
125
150

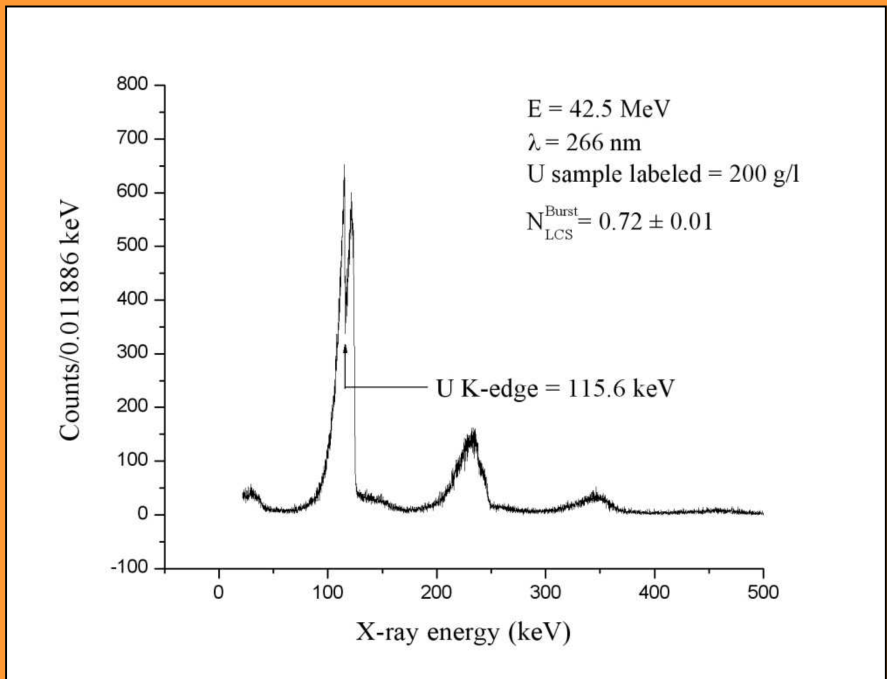
E = 42.5 MeV
λ = 266 nm
U sample labeled = 200 g/l
N_{LCS}^{Burst} = 0.72 ± 0.01
U K-edge = 115.6 keV
Counts/0.011886 keV
X-ray energy (keV)
800
700
600
500
400
300
200
100
0
-100
0
100
200
300
400
500

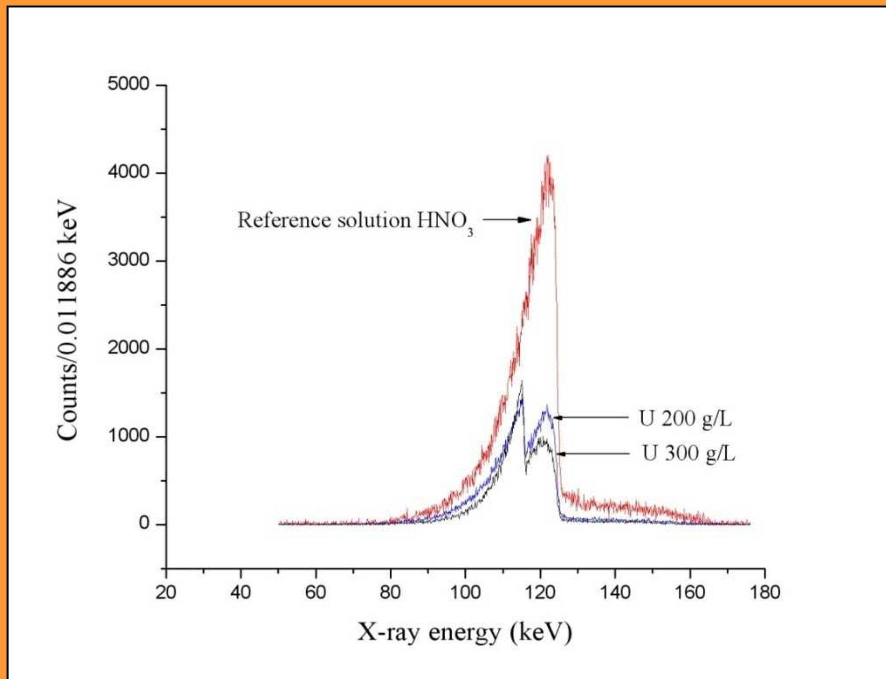
Reference solution HNO_3
U 200 g/L
U 300 g/L
Counts/0.011886 keV
X-ray energy (keV)
5000
4000
3000
2000
1000
0
20
40
60
80
100
120
140
160
180

Concentration measurements

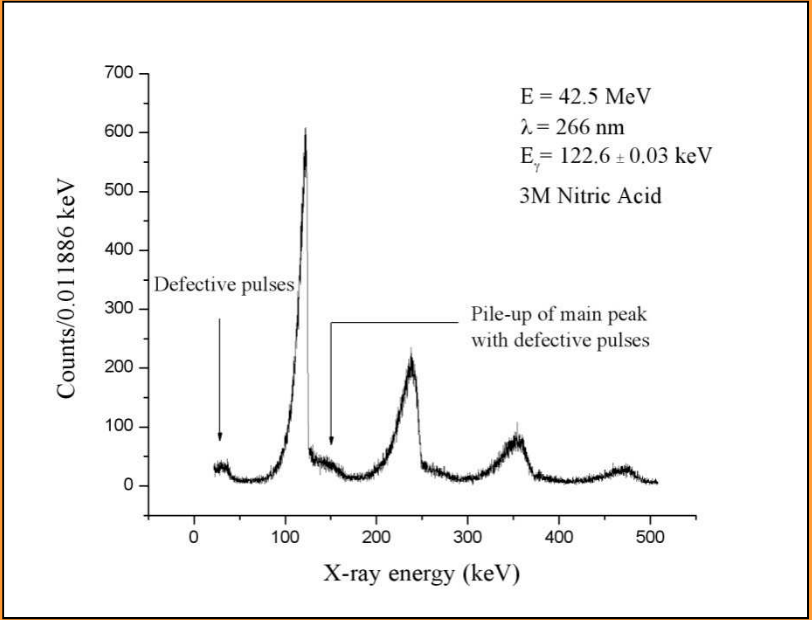

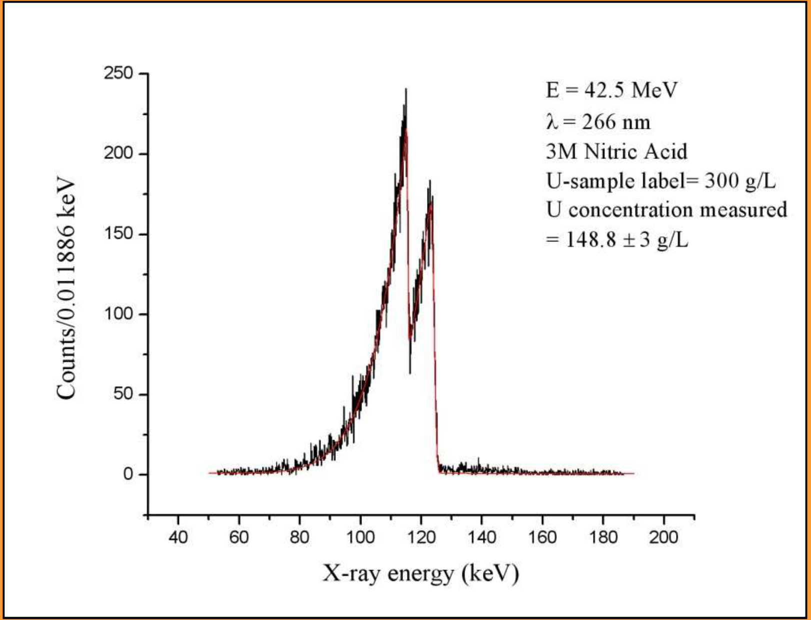

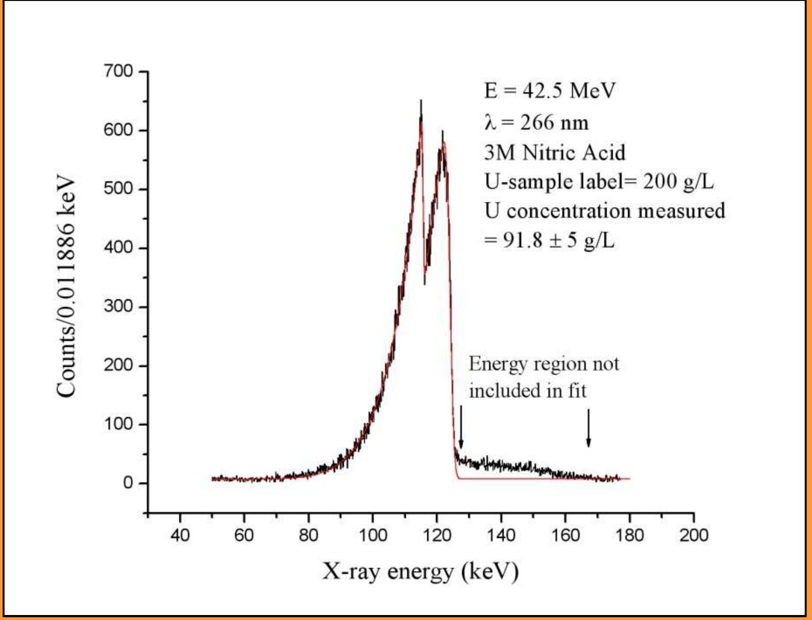

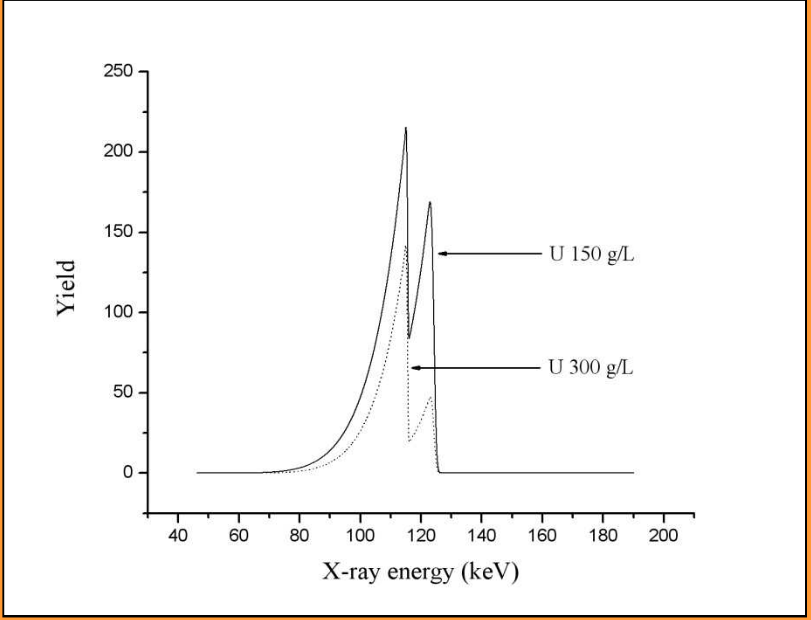

Polarized x-rays: XRF, Material science i.e. magnetic Compton scattering, x-ray magnetic dichroism (XMCD), x-ray diff optics.

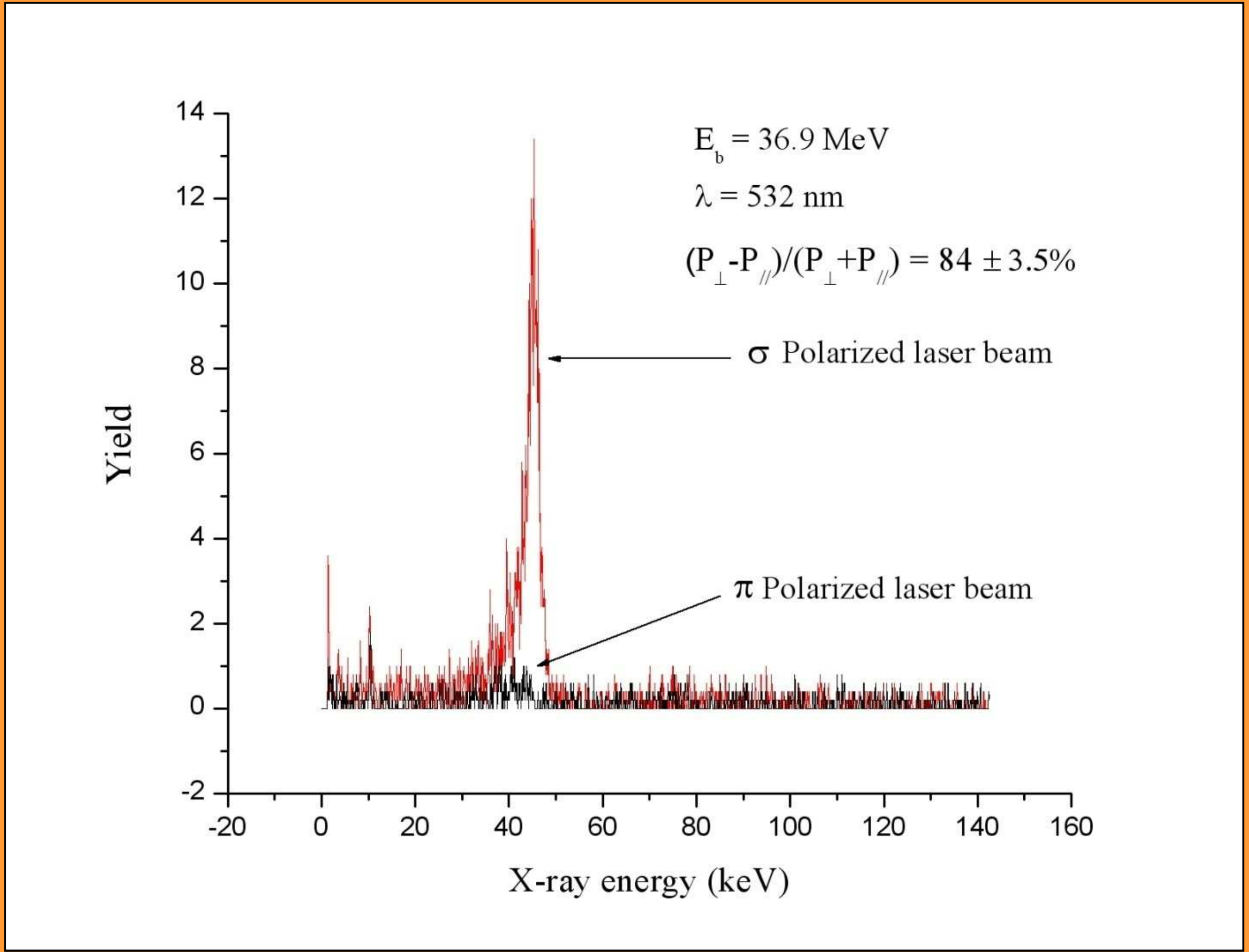

Fixed detector position at 90° with respect to scatterer

Main goal:

1-Determination of detection limit of actinide elements concentration that can be reached with LCS x-rays and comparison with x-ray tubes (1mg/l up to about 300 g/l).

2- U/Pu sample 200g/l-1g/l

3-TRU product

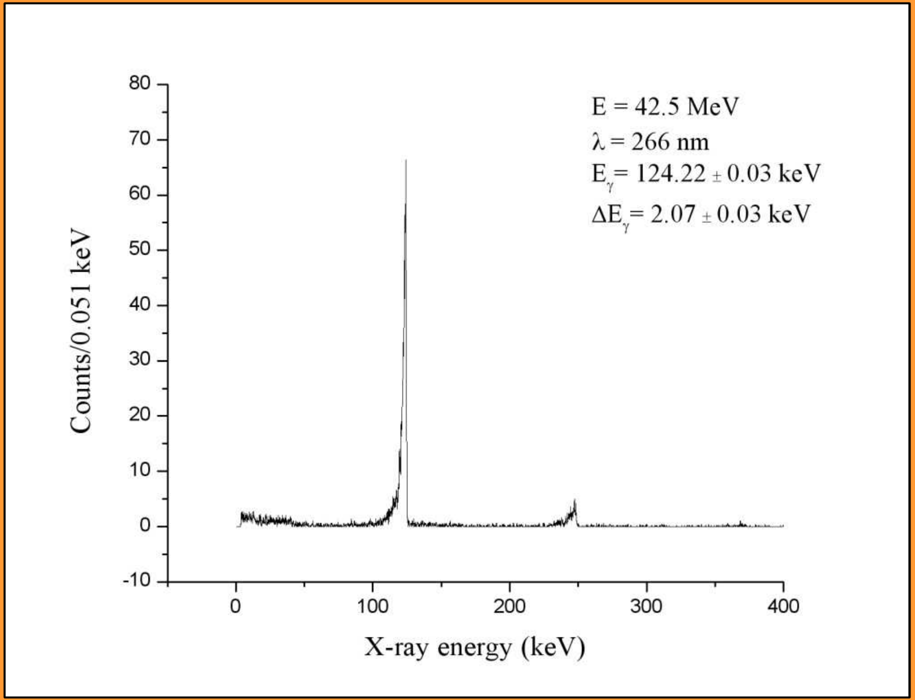

Bio-Medical Imaging

Production of high-quality images of soft tissue while reducing dose.

Typical x-ray yield = 10^7 photons/cm^2 and $\Delta E \leq 5\%$.

Conventional X-ray source

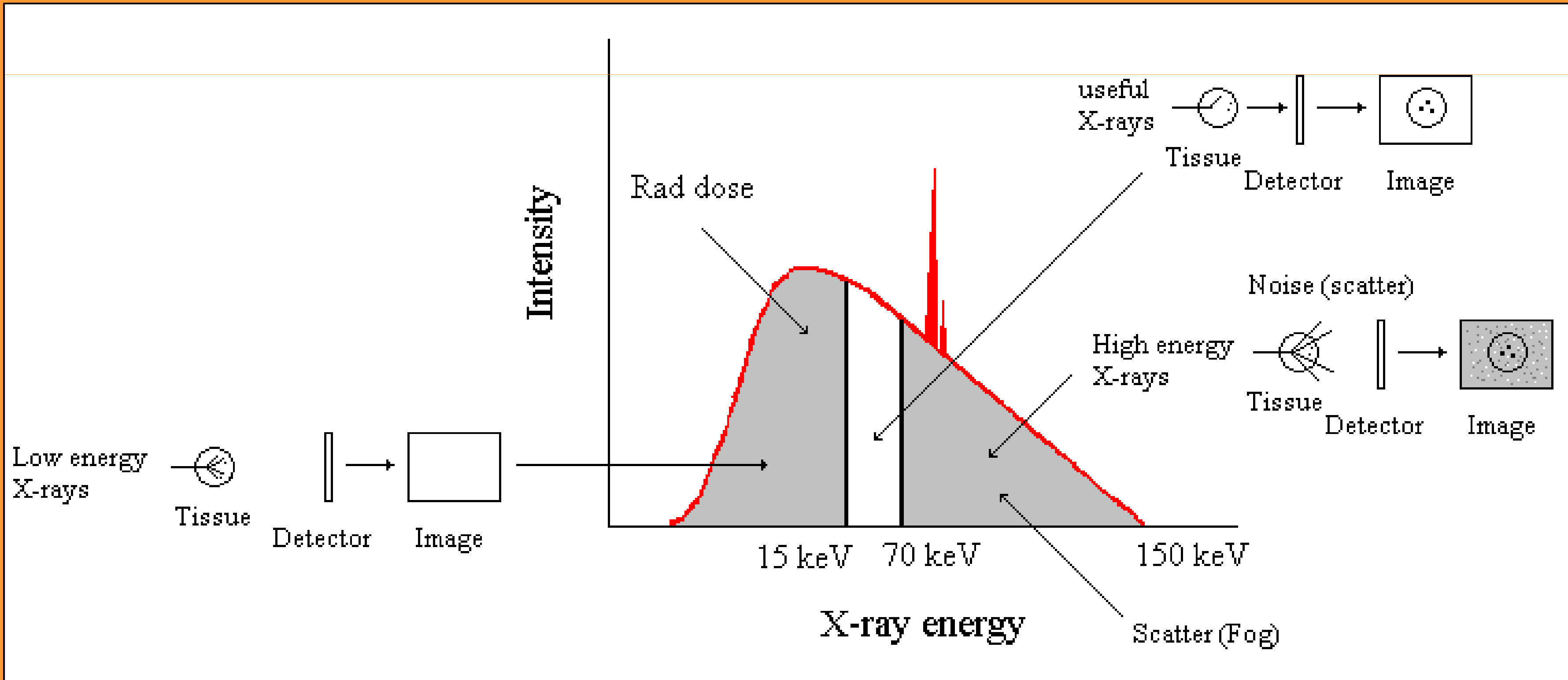

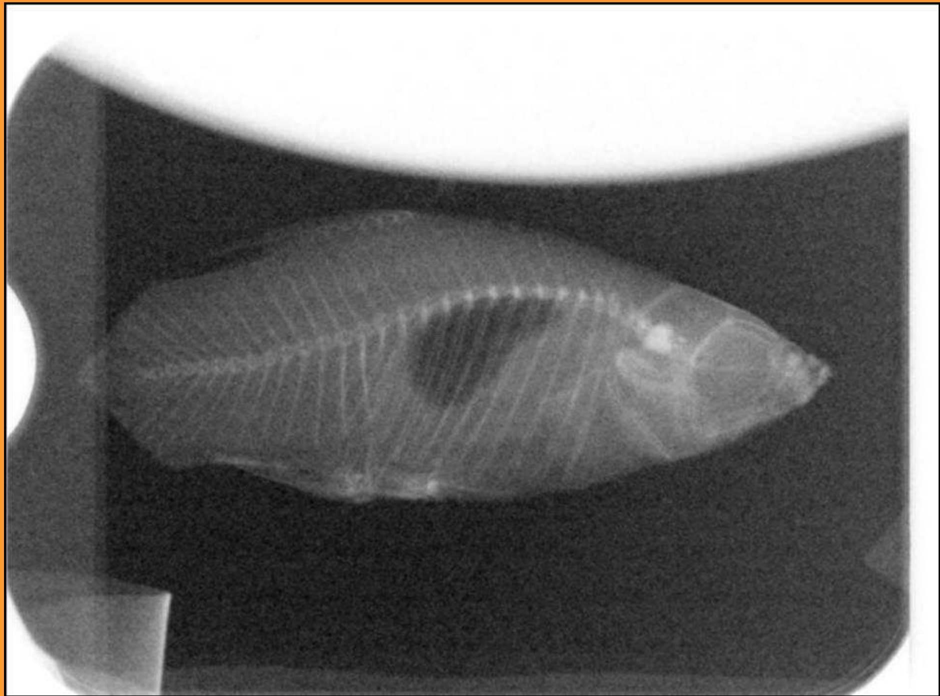

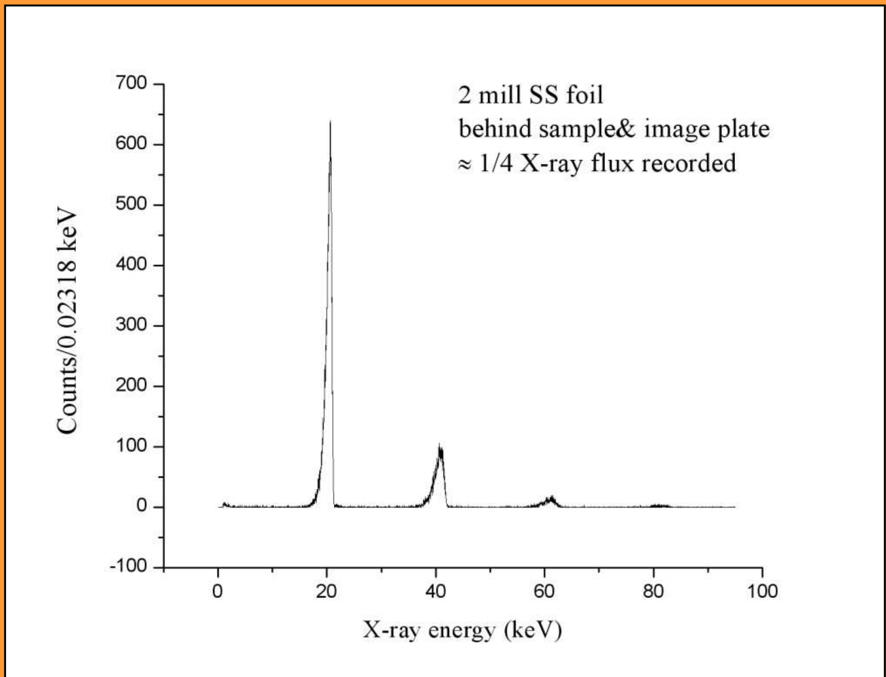

Gendex dental plates

1064 nm laser wavelength.

X-ray energy = 20 keV.

Fish-X-ray flux: ≈10^4 Ph/mm^2

Mouse- X-ray flux:

≈10^5 Ph/mm^2

LCS X-ray beam image

Off axis emission ➔ Factor >4 loss in X-ray yield

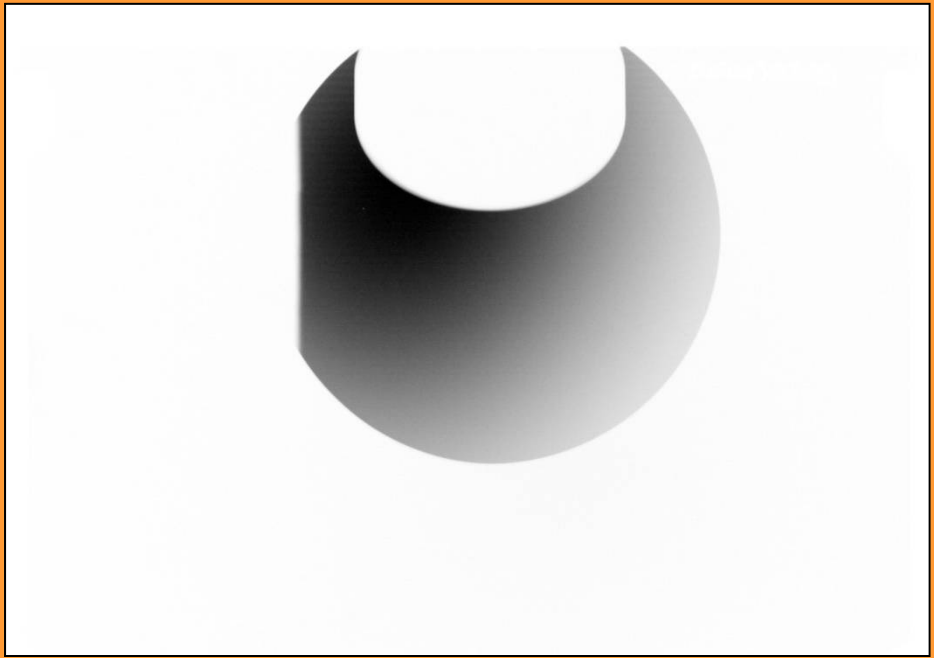

Phase imaging (bottle cap)

Laser (1064 nm) spot size:

$\sigma \approx 180\ \mu m$ (need tighter beam focus)

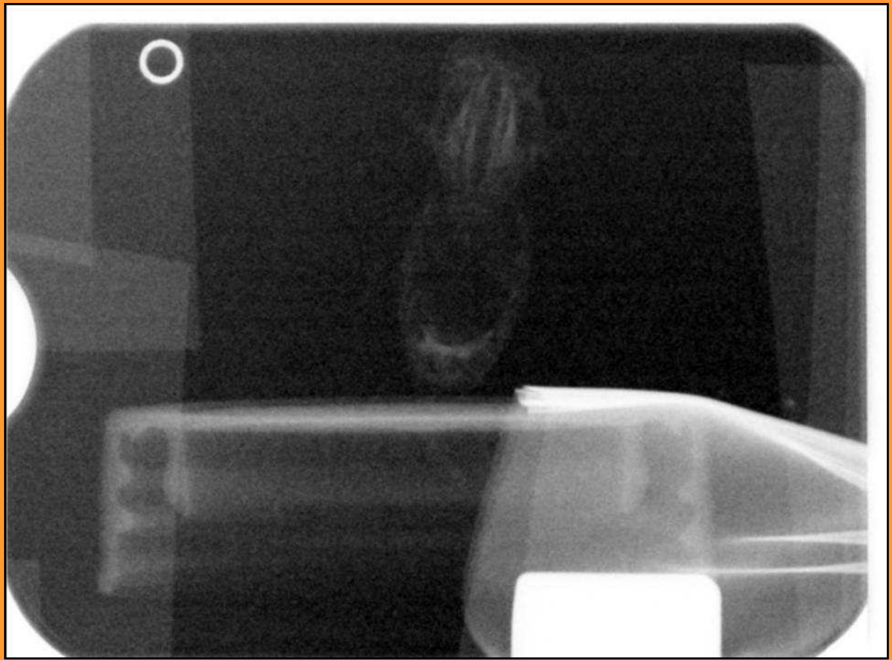

X-ray image of memory stick at X-ray energy ≈ 47 keV (532 nm). Dimensions = 1.5x3.5cm

Total flux ≈1.2×10^5 Ph/mm^2

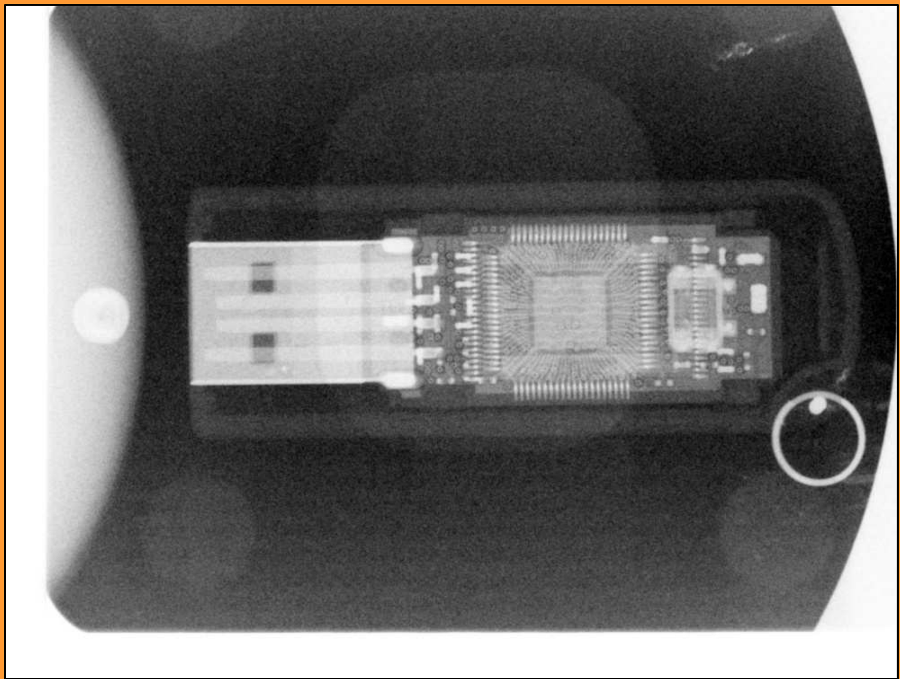

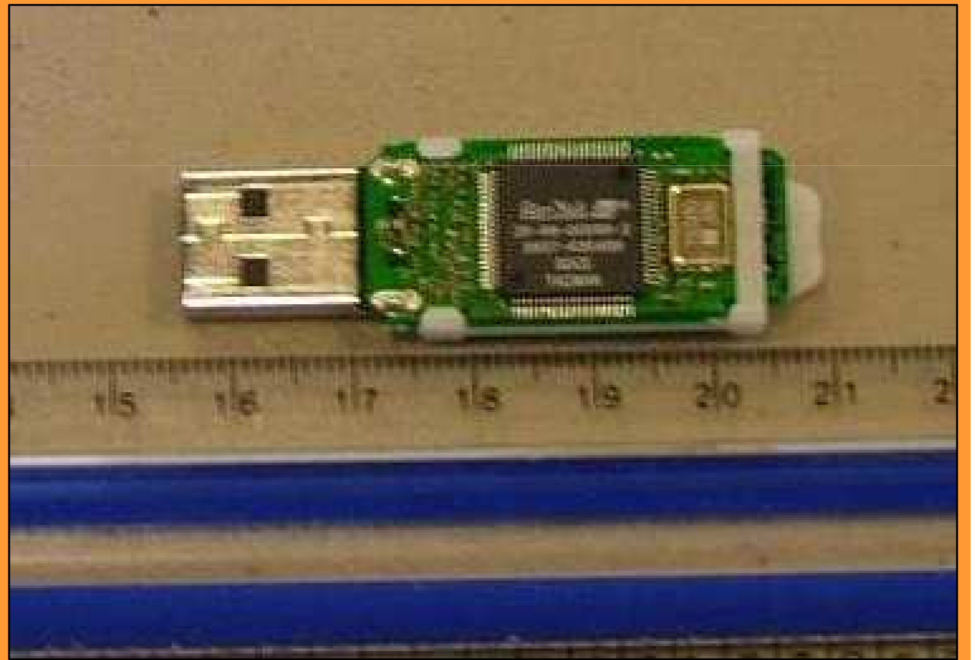

Spatial resolution ≈ 12 Lp/mm

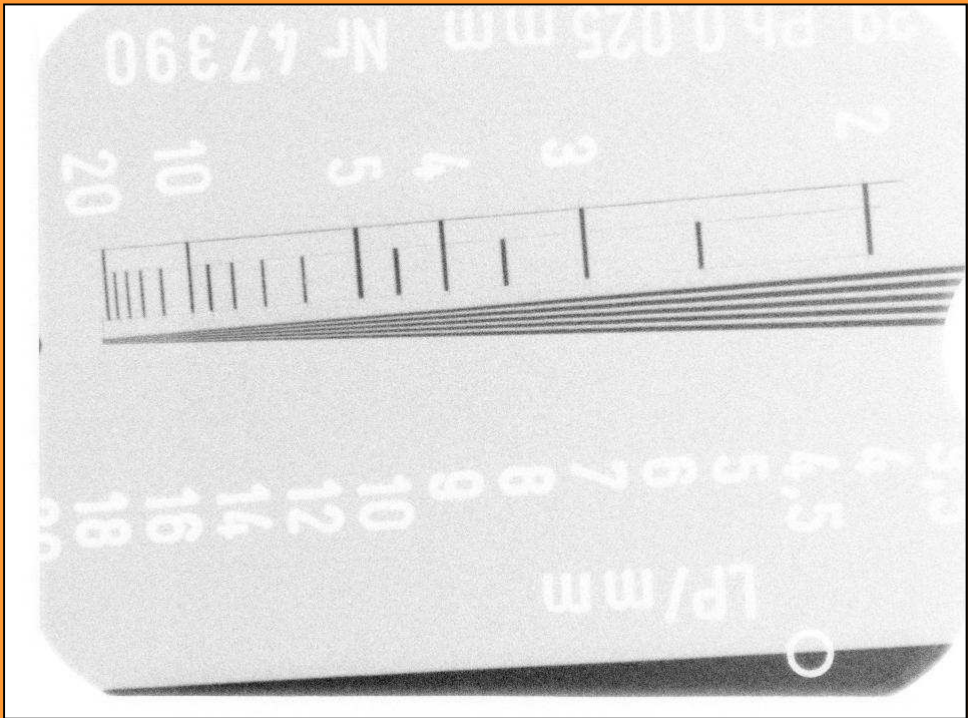

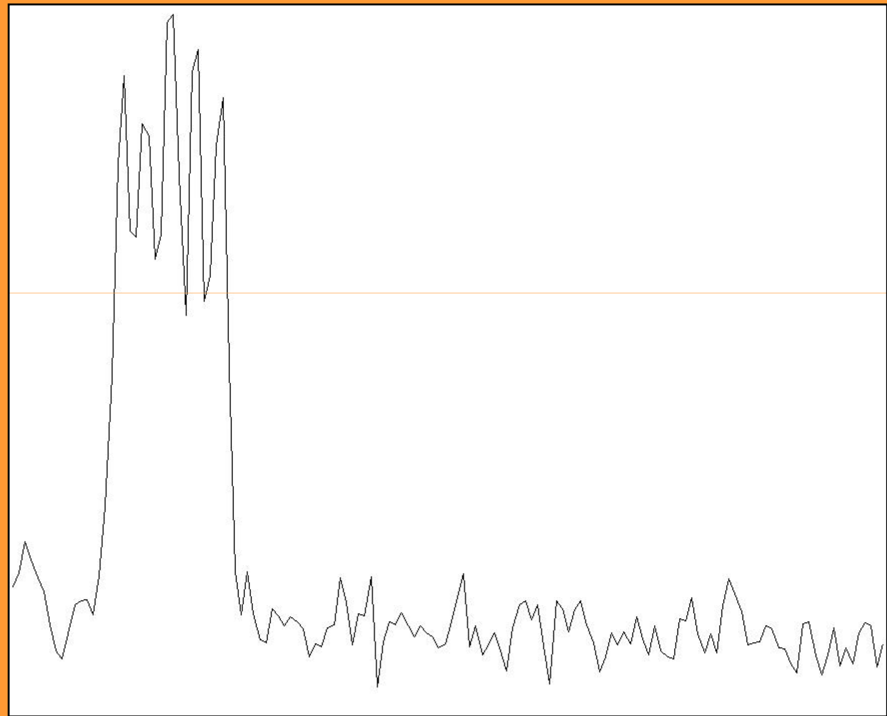

Future goals

•Comparison of LCS and OTRI.

OTRI: $\sigma \approx 0.01/\gamma$

Limitation: Low energy e-beams and high quality e- beams due to scattering in first foil.

• (x,x') e^- mapping

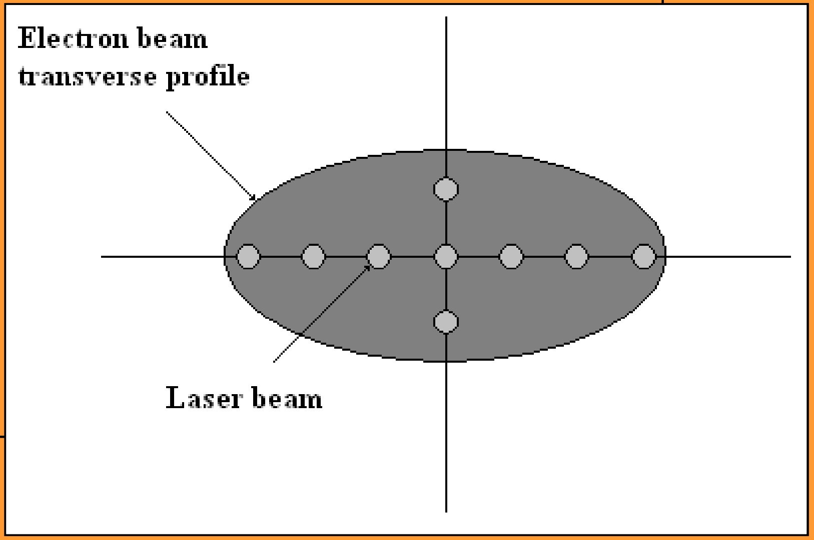

Single shot beam diagnostics with LCS

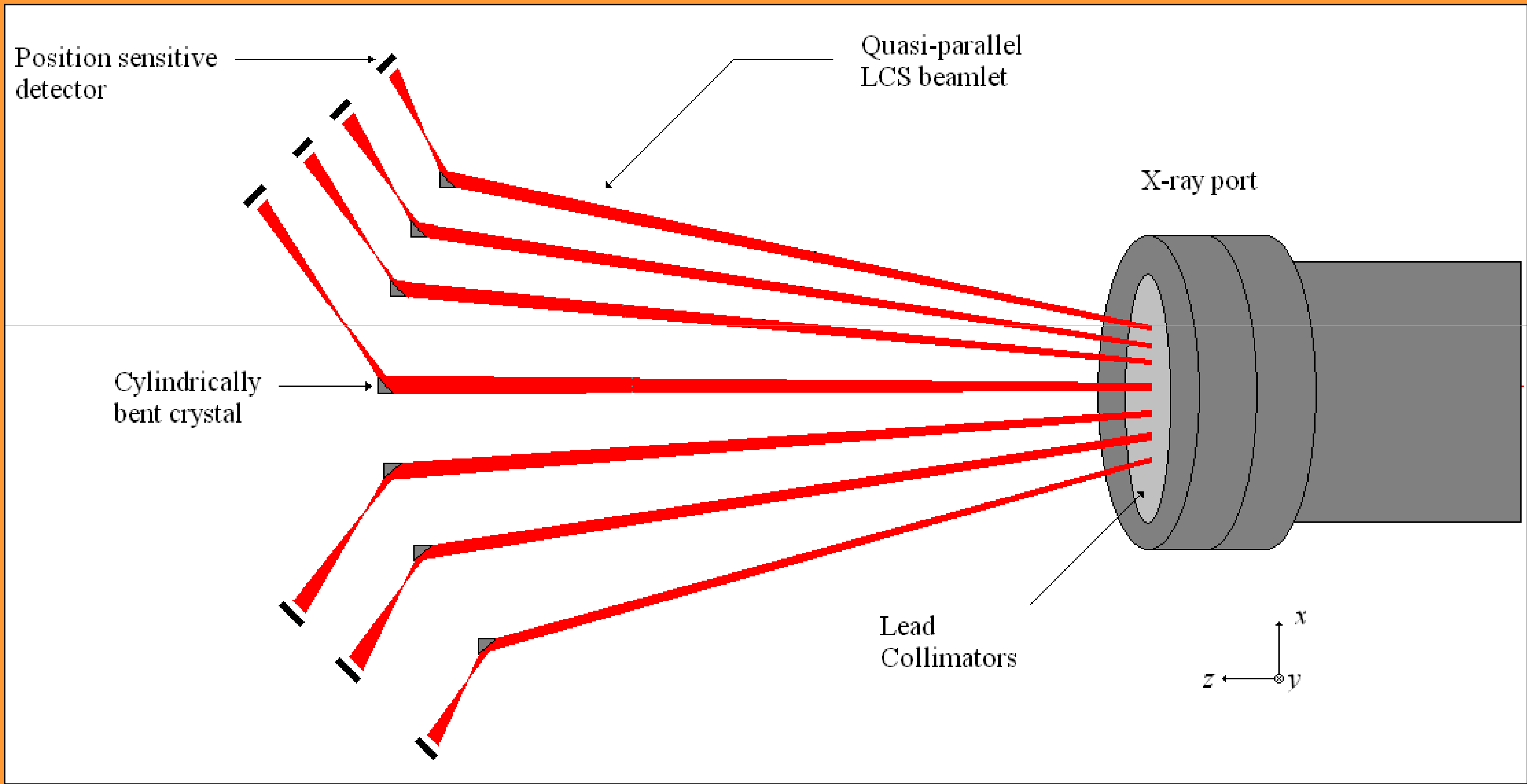

Conclusion

LCS can be a versatile x-ray source provided that one has the necessary yield!

LCS has a wide range of applications in accelerator physics,bio-medical field, material sciences and non-proliferation.

LCS projects of interest at IAC:

*Proof of principle of single shot electron beam diagnostics, transverse phase space mapping and comparison of LCS to other developed diagnostic techniques such as ODTRI, R. Fiorito (UMD).

*HKED with U/Pu, Dissolver solution (U/Pu/Np/Am/Cm) and TRU (Pu/Np/Am/Cm), M. Collins (LANL) and B. Cipiti (Sandia).

*Image contrast/ X-ray dose VS LCS X-ray energy and bandwidth.

*Phase/Absorption imaging: Low Z materials embedded in soft Tissue, E. Ritman (Mayo clinic), M. Gambaccini and A. Taibi, (Univ. of Ferrara, Italy).